

VĚDECKÉ SPISY VYSOKÉHO UČENÍ TECHNICKÉHO V BRNĚ

Edice PhD Thesis, sv. 861

ISSN 1213-4198

thesis IS

Ing. Jakub Cejpek

**Analysis of Aeronautical
Composite Structures
under Static Loading**



FACULTY OF MECHANICAL ENGINEERING

INSTITUTE OF AEROSPACE ENGINEERING

**ANALYSIS OF AERONAUTICAL COMPOSITE
STRUCTURES UNDER STATIC LOADING**

**ANALÝZA KOMPOZITNÍCH LETECKÝCH KONSTRUKCÍ
PŘI STATICKÉM ZATÍŽENÍ**

SUMMARY OF DOCTORAL THESIS

OBOR	Design and Process Engineering
AUTOR PRÁCE	Ing. Jakub Cejpek
ŠKOLITEL	doc. Ing. Ivo Jebáček, Ph.D.
OPONENTI	doc. Ing. Jaroslav Juračka, Ph.D. Ing. Bohuslav Cabrnock, Ph.D.
DATUM OBHAJOBY	22. června 2018

Brno 2018

Keywords:

Composite component analysis, finite element analysis, beam theory, landing gear spring, wing spar.

Klíčová slova:

Analýza kompozitních komponent, konečnoprvková analýza, nosníková teorie, pružina podvozku, nosník křídla.

Místo uložení:

A copy of the dissertation thesis is available at the department for Science and Research, Faculty of Mechanical Engineering, BUT.

Rukopis dizertační práce uložen v Oddělení pro vědu a výzkum FSI VUT v Brně.

© Jakub Cejpek, 2018

ISBN 978-80-214-5682-2

ISSN 1213-4198

Contents

1	Introduction	5
2	Literature review	6
2.1	Product	6
2.2	Material	6
2.3	Computer Aided Design and Engineering	8
2.4	Industry problems and Goals of the Dissertation Thesis	10
3	KuFEM	11
3.1	What is KuFEM?	11
3.2	User input	12
3.3	Analysis work-flow and equations	15
3.4	Output functions	25
4	Practical examples of KuFEM results	26
4.1	HPH Shark Composite Wing	26
4.2	Main Landing Gear Spring of Merlin 103	28
4.3	Nose Wheel Spring of Merlin 103	30
4.4	Tail Gear Spring of Merlin 110	33
5	Summary and Conclusion	35
5.1	Meeting the dissertation goals	35
5.2	Contribution and novelty of the thesis	36
5.3	Final conclusion	36

1 Introduction

Composite materials have gone a long way in the last half a century. May the new wide body airliners be the proof of the advancements the science and industry has achieved on the fields of design, manufacturing, maintenance and life cycle control.

Compared to the state of the art products from industry giants Airbus and Boeing, the state of affairs in the small companies, producing light sport airplanes is very different. These companies are not even close in terms of budget and possibilities.

The design process requires material data in order to estimate the stiffness and predict a failure that is likely to occur. These data should be obtained through conducting a large number of different test, that will determine the strength and stiffness of a specimen, that represent the final product (manufacturing process, fibre volume fraction, waviness, foreign objects, gas bubbles and so on). From these laboratory data the material model can be built and only after this is achieved, the part can be actually designed.

Described process takes a lot of time, man power and is expensive. Small companies can not afford to choose this long road in their designs, at least not to the full extend.

It is the author's experience that small companies choose different approach.

Motivation

The author took part in design, analysis and testing of landing gear springs at TechProAviation company. Another experience is drawn from HPH glider wing analysis conducted at the Brno University of Technology.

The experience from these projects convinced the author to focus on the topic of thick composite structures (landing gear spring and wing spar, figure 1.1) and methods of their analysis.



Figure 1.1: Example of aeronautical structures: wing and spring landing gear.

Today's practice in design is either simple closed-form analysis approach or rather lengthy and costly finite element analysis. Neither method is optimal. Third option should exist: thorough analysis and yet efficient, fast and flexible.

There is a number of software tools, developed at universities or commercial companies, that are - in their area - just the right compromise between simple tool and bone deep analytical software. Such narrow oriented programs are, for example, Glauert, MITCalc and ministatic.

Summary

Companies based in Czech aviation industry usually can not afford expensive software, spend long time on multiple variant analyses or number of specimen tests. These companies might take an advantage of a simple program, dedicated to calculate just one type of product. The chosen typical product is landing gear spring or, to some extend, wing spar.

The chosen product is a slander thick composite beam of varying rectangular cross-section, with dominant bending loading. Significant curvature of the geometry and large deformations are typical. Usually the composite layup is unidirectional with few wrap layers of $\pm 45^\circ$ plies.

This thesis's goal is to suggest and provide the means for better analysis of composite parts, namely the landing gear springs.

2 Literature review

Following text is a summary of the pre-requisites for the original work. This summary is the starting point for the main work, which is presented in the subsequent chapters.

2.1 Product

The subjects to have potential benefit from this thesis are companies that need fast, reliable and easy to use program for their composite products. Program is focused to landing gear spring design for small airplanes (under [25], [26], [24] and [27] regulations). However this is not the limit: other products (such as wing spars) may be analysed also.

2.2 Material

The wing spar (flanges) and landing gear springs are classified as thick composite structures. Therefore the focus of this thesis is on the thick composite material based on unidirectional lay-up. Following information is taken from [15], [9], [18] and [11].

One definition of *thick* is based on the Mindlin–Reissner plate theory, which is through the plate thickness-to-width ratio greater than 10%. Other definition marks the composite as thick if it contains over 15 plies.

However the most important property of the thick composite is the out-of-plane stress. By through-thickness loading new phenomena occur, such as ILSS. Therefore the appropriate attention should be given to the analysis of these effects.

- **Material properties**

Total of five independent material constants are needed for strain vector determination. The following suggestion defines E-glass fibre unidirectional composite in terms of these constants.

- Lateral and through thickness modulus

It has been established, that $E_2 \equiv E_3$. In the beginning of the analysis, with no better data, the elastic modulus of the matrix can be used: $E_2 \equiv E_3 = E_M$.

- Longitudinal modulus

Longitudinal modulus is mostly based on the fibre volume fraction and fibre elastic modulus. For E_1 value following estimation can be used:

$$E_1 = E_F \cdot V_F + E_M \cdot (1 - V_F)$$

- Poisson's ratios

Typical value of isotropic metal material is $\mu = 0.3$. Similar values are usually published for composites: $\mu_{12} = (0.23 \div 0.30)$ [15], [16].

Poisson's ratio in the plane, perpendicular to the longitudinal direction, can be approached in similar way as out-of-plane elastic modulus: only the matrix matters. Therefore $\mu_{23} \equiv \mu_M$.

- **Hook's law for thick unidirectional composites**

Hook's law defines the relationship between stresses and strains of the material. After the analysis, which compares actual numbers for the intended application (that is landing gear springs and wing flanges), the following simplification can be made:

$$\epsilon_1 = \frac{1}{E_1} \cdot \sigma_1$$

- **Unequal tensile and compression properties**

A short assessment of the *MR* ratio is based on data collected from [28], [19],[17] and [15]. These data suggests that the difference in tensile and compression moduli is between 2 – 5%. This difference is quite low. However the author feels that this difference should not be omitted in the analysis.

- **Failure criteria**

When designing a new product - for example the main landing gear - a good question is what failure is likely to occur? It is shown on figure 2.1, that the loading bears similar¹ character as the tree-point-bend test.

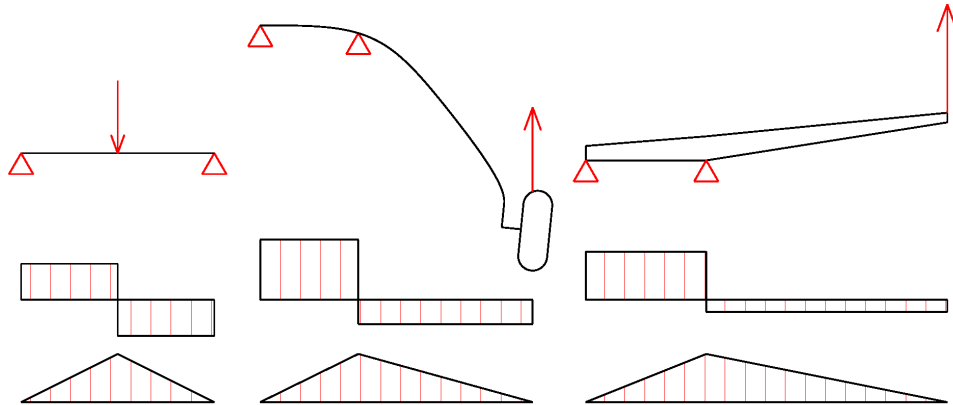


Figure 2.1: The similarity between three-point-bend test, landing gear and wing loading character.

Mr. Davallo [20] performed a number of flexural tests of wet layup laminates. All of these samples have failed in the same way: delamination. A number of failed landing gear springs at TechProAviation exhibits this very same failure. Other common failure observed during the drop tests is the result of through-thickness stresses. These failures are shown on figure 2.2.

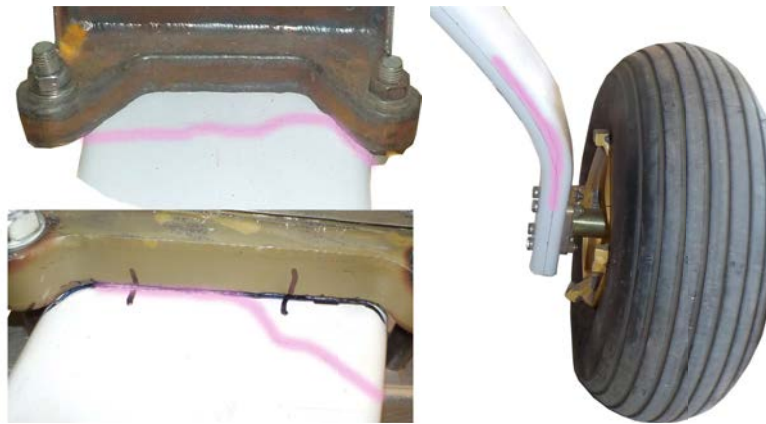


Figure 2.2: Typical landing gear failure: delamination and through-thickness crashing.

This thesis focuses on the products that are mostly loaded by simple bending. For this loading maximum strains or maximum stress will be adequate failure criteria. However, just like in three-point-bend test, there is an area where extensive through-thickness force is introduced. At this point a special analysis considering the through-thickness stress will take place. Also the issue of delamination exist, especially in the curved (small radius) areas.

- **Laboratory test experiments**

In the intended area of application the coupon tests are expensive, impractical and therefore redundant. Omitting coupon tests leads to a practice of testing the component as it is. This practice however brings some drawbacks.

¹For the illustrative purposes only the dominant force is considered.

The article [23] illustrates another drawback of omitting the coupon testing. Only 50% load has been applied during the laboratory test. The reason for this is that the specimen must not be destroyed. Probably, the specimen will be later used for the drop test of the whole airplane. Such test provides only the stiffness characteristic (force-deflection dependency). Not achieving the failure results in the lack of failure data for the material. Thus no validation of failure criterion can be evaluated, because no relevant data were obtained.

2.3 Computer Aided Design and Engineering

Old schema of a company with separate design and analysis departments has changed during the last decade. New trend shifts the basic conceptual analysis directly to the design department, while the analysis department focuses on special, more thorough studies.

This shift has been enabled by combining CAD and CAE system into a single program distribution. Well known leading companies are Dassault Systèmes and Siemens. Their programs allow user to interact with 3D model and FEM in real time.

There are two other types of FEA programs. Both are dedicated only to analysis (there is either no 3D modeller at all or one with very limited capabilities). First types are the universal FEA programs, such as Abaqus, ANSYS and NASTRAN. Other programs are specialized and far less sophisticated, for example Ministatik.

In the author's experience it is not very common for FEM software to allow deformed geometry exports in a format, that can be used for perturbation or clearance analyses. To some extent the CAD built-in CAE modules allow these tasks. But only recent version (for example ANSYS 17 [10]) introduced a functionality that exports STL or STA file with deformed geometry.

• Beam and Plate Theories

There are three basic beam theories: the oldest and most basic Euler-Bernoulli formulation, advanced Timoshenko formulation and quite complicated second order formulation. Similar situation is with the plate theories, which were developed from the beam theories.

Even though the plate theories, especially the higher order theories, offer great features in thick composite analysis, they are not suitable for achieving the goal of this thesis. The reason are: difficult formulation in comparison to the beam theories and geometrical limitation of 2D analysis (plate element would have to be turned 90°). Both, the Euler-Bernoulli and Timoshenko theories are adequate tools in solving chosen composite components.

• Programming language

Mr. Ferreira [1] uses Matlab scripting language for its easy-to-understand appearance and capability to work easily with matrixes.

Indeed Matlab is very useful language with many practical capabilities. However several issues exclude Matlab from being used in this thesis do exist. It is not a freeware. Second problem concerns GUI. In order for a software to spread into public general use, it must be user-friendly. One of user-friendliness keystones is the graphical user interface.

Stand-alone capability (executable program) is very important to any software. It allows simply run the application on any computer without having to think about other supporting programs.

Python language is very popular among engineers lately [29]. It provides large libraries, such as Numpy [33] specialized to mathematical operations. GUI can be built easily with WX-Python library [34]. And Py2EXE library [35] can be used to develop a stand-alone executable application.

• Deformation, Deflection and Displacement

The author makes an effort throughout this text to use these terms in the meaning explained bellow. The explanation is based on [14]. Figure 2.3 shows the difference between deflection and displacement.

Deflection is the distance that an object bends or twists from its original position. Deflection is a general term that refers to a shape that the object transforms to when external loading is introduced.

Displacement is a vector that quantifies the deflection. In general, there are six constituents

of a displacement vector (three translations and three rotations).

Elastic **deformation** is a resulting distortion in the material. It is the result of the force introduced externally. Deformation is equivalent to the term **strain**.

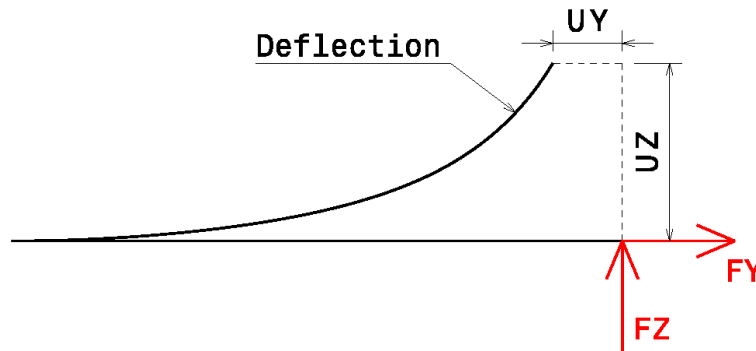


Figure 2.3: Deflection and $[U_Y, U_Z]$ displacement.

- **Non-linearity**

There are several types of non-linear behaviour, that may affect the solutions: material (plasticity, creep); boundary conditions and loads (springs, etc) and geometry, according to [6] and [13].

Geometrical non-linearity is in the context of this thesis of most interest. Large deformations are expected in case of main landing gear. This expectation is illustrated on figure 2.4 showing a drop-test of Merlin 100 airplane. This figure is composed from a picture with un-deformed landing gear and the maximum deformation. The direction of the loading may not change (flat surface). However the arm of the force changes with the displacement.



Figure 2.4: Composed picture of main landing gear during drop test. Un-deformed and maximum deformation. Courtesy of TechProAviation, s.r.o.

- **Verification and Validation**

Any mathematical model needs to be validated and verified in order to be considered credible. Verification of a finite element analysis confirms, that the used model is correct. For the purpose of KuFEM verification, the following definition is adopted:

"KuFEM is considered to be verified if the calculated results are same or very close to closed formula results and NASTRAN outputs."

Usually, validation of a mathematical model is achieved through the calibration. Which is a comparison of the model and actual measurement. This effectively means:

"KuFEM is considered to be validated if the calculated results are close to actual laboratory measurement."

This definition may prove to be controversial. It expects a perfect product and perfect measurement. Therefore multiple measurements will have to be made in order to obtain statistically significant results.

2.4 Industry problems and Goals of the Dissertation Thesis

Current problems

- Industry problem:
 1. The Czech Republic is a large producer of small sport airplanes.
 2. These airplanes commonly use thick unidirectional composite components for landing gear.
 3. Practically all composite parts in this sector are made by wet layup.
 4. These composites are far from perfect.
 5. Thick composite parts can be manufactured in precise moulds with good control over the volume fraction.
 6. If the volume fraction can be controlled reliably, the stiffness can be determined accurately.
 7. Stiffness of the composite affects the deformation characteristics.
 8. Landing gear springs exhibit large deformations in one plane.
 9. Means of analytical analysis are not sufficient and effective tools in the landing gear design.
 10. Small companies rarely own software and know-how deep enough to do effective landing gear design.
- Commercial Structural Analysis Software:
 1. Available software² is universal.
 2. It takes a long time to understand and operationally use such software.
 3. This kind of software is expensive.
 4. The time to build, evaluate and optimize a FE model is too long.
 5. The more precise the model, the less flexible it becomes.
 6. Exporting of the deformed shape is not a native function to current software.

Goals

- Develop a program, that will:
 1. be used in design and analysis of typical thick composite parts,
 2. predict displacements in one plane,
 3. calculate the element loads, stresses and strains,
 4. export these results in understandable fashion,
 5. be easy and flexible to use,
 6. allow user to export geometry of deformed body,
 7. allow user to export NASTRAN BDF file.
- Verify and validate the software

²This point considers dedicated FEM softwares (Ansys, Abaqus, etc).

3 KuFEM

Previous chapters revealed that thick composite structural parts are commonly used for small airplanes. Whether it is main landing gear, nose or tail gear spring or even main wing spar, all the parts are similar in terms of material behaviour, loading and deflection characteristics. In each case there is one dominant direction of loading and deflection. In this direction the largest and most significant displacement exists. Also the boundary conditions are similar (three-point bending is often encountered). Forces and displacements, perpendicular to the main loading direction, do exist. But these are not as significant as those of primary direction. For this reason only planar deformation analysis should be sufficient enough.

3.1 What is KuFEM?

KuFEM is a program with a graphical user interface (see figure 3.1) for predicting deformed shape of a structural part and evaluating the stresses and strains. It is being developed with composite specifics in mind in order to evaluate more than just simple tension/compression. KuFEM allows simple export of deformed geometry (shown on figure 3.3) so the user can quickly evaluate collisions in his 3D model.

The software is based mostly on [1], [2], [3], [4], [5] and [7].

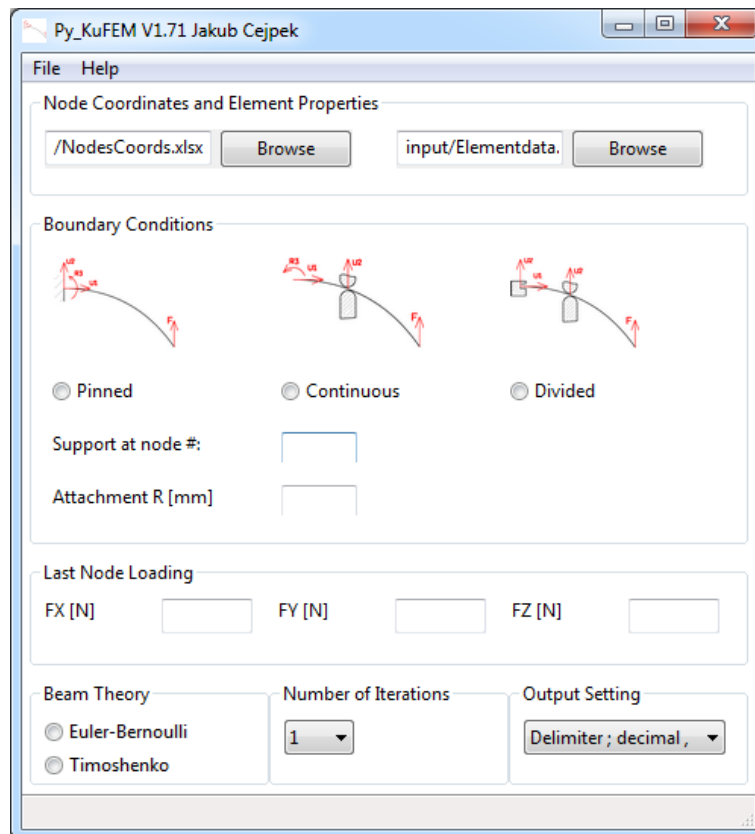


Figure 3.1: Graphical User Interface (GUI) of Python-built version of KuFEM.

Principle, how the program works, is shown on diagram 3.2. User is supposed to prepare the analysis input data, which consist of: geometry, boundary conditions, loading and calculation setting.

Based on these data, provided in the form of a spreadsheet tables, field inputs and radio-boxes in the GUI the deformed shape is predicted. Upon this deformed shape the forces and moments

are calculated along the length of the model. Then the stresses and strains are calculated. When the program is finished with the calculation, the results are exported. These results are presented in three forms: detailed text file, spreadsheets and IGES geometry.

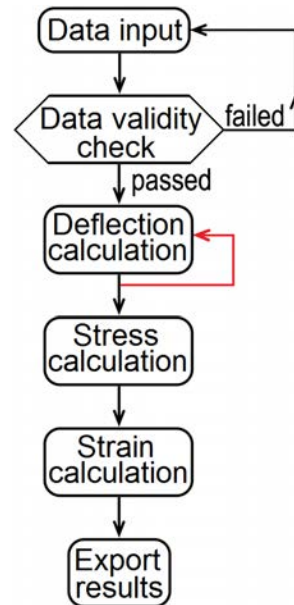


Figure 3.2: Basic diagram of the program.

User is also allowed to generate a BDF file (NASTRAN input file) that allows him to run very similar analysis in NASTRAN solver. This option provides an opportunity to verify the KuFEM results.

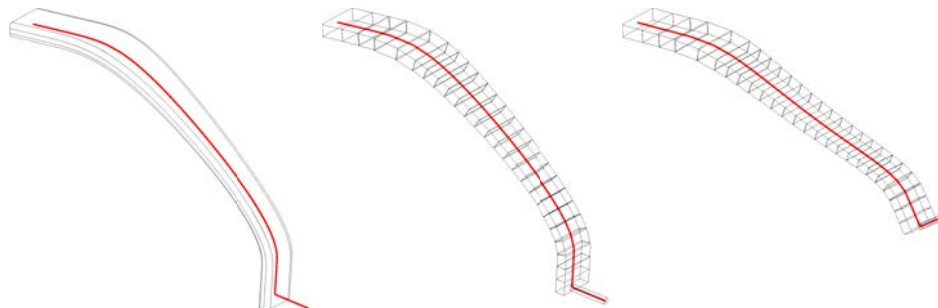


Figure 3.3: Original geometry. Meshed un-deformed geometry. Predicted deformed geometry.

3.2 User input

Program inputs are in two forms: spreadsheet files describing geometry and various settings and values in the graphical user interface (GUI). All inputs are described in detail in the following paragraphs.

3.2.1 Spreadsheet data

NodesCoords spreadsheet

First, user is required to define the mid-fibre of the model. The mid-fibre is created as an intersection of two planes representing geometrical centre of the thickness and width along the

length. In case of the main landing gear the last node is the centre of the wheel.

Having the mid-fibre defined, user must mesh the curve. Keep in mind that there should be node at each significant area, such as boundary condition, geometry change or different properties (this may be even more significant for composite structures as a stiffness may rapidly change). Node coordinate input can be found on figure 3.4

Total number of nodes should be high enough to represent the curved geometry and yet low enough for user's sake. For example main landing gear for Dusty and Merlin airplanes used 25 and 31 nodes respectively. In similar analysis [21] a total of 33 nodes were used. The size of the array is $2 \times \text{noNod}$, where noNod is a variable denoting the total number of nodes.

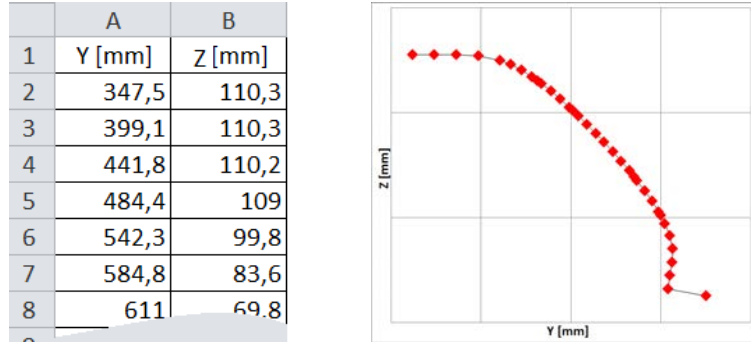


Figure 3.4: Spreadsheet example. Graphical representation of the spreadsheet values.

ElementData spreadsheet

Each two neighbouring nodes form one beam element (shown on figure 3.5). Therefore:

$$\text{noEl} = \text{noNod} - 1 \quad (1)$$

ElementData spreadsheet defines the geometrical and mechanical properties of each element

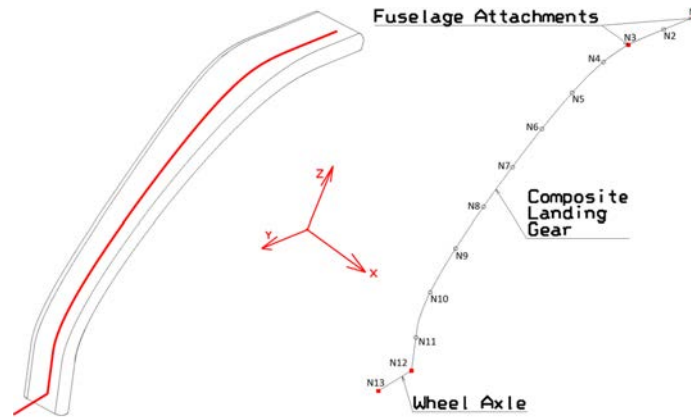


Figure 3.5: Nodes and elements iso-view.

(explained on figures 3.6 and 3.8). These values are:

- $B[mm]$ width,
- $T[mm]$ thickness,
- $t_H[mm]$ upper flange thickness,
- $t_D[mm]$ lower flange thickness,
- $E_H[MPa]$ upper flange stiffness,
- $E_D[MPa]$ lower flange stiffness,
- $t_O[mm]$ wrap thickness.

	A	B	C	D	E	F	G
1	B [mm]	T [mm]	TH [mm]	TD [mm]	EH [MPa]	ED [MPa]	tO [mm]
2	98,38	26,48	8,2	8	52500	68000	0,99
3	98,81	26,46	8,2	8	52500	68000	0,99
4	101,47	26,39	8,2	8	52500	68000	0,99
5	105,86	26,33	8,2	8	52500	68000	0,99
6	106,78	26,29	8,2	8	52500	68000	0,99
7	103,87	26,12	7,8	7,6	52500	68000	0,99
8	100,33	25,79	7	6,8	52500	68000	0,99
9	96,57	25,38	6,6	6,4	52500	68000	0,99

Figure 3.6: Element data spreadsheet table.

3.2.2 Boundary conditions

User can choose from three different boundary conditions. This option increases the potential of the program. User can choose from the following boundary conditions: pinned, continuous and divided.

These boundary conditions represent the most typical clamping and support combinations encountered in relation to the wings and landing gear springs. Further description follows in section 3.3.4.

3.2.3 Loading

Last node loading allows user to input the vector of forces in X, Y and Z direction. As the analysis is only 2D in terms of deformation, but 3D in terms of stress (strain) distribution. Force in the X direction will produce no deflection in this model.

3.2.4 Beam theory

Two beam theories are available for user to choose from. The choice will only affect the deflection (Timoshenko definition introduces shear effects. Therefore it is not as stiff as Euler-Bernoulli).

Choice of beam theory has no direct influence on stress / strain values. Further information on the beam theory implementation is given in section 3.3.2.

3.2.5 Number of iterations

Section 2.3 shows that the landing gear deflection is extensive and geometrically linear analysis may not be suitable for this kind of problem. For this reason a simple procedure of step-by-step load increase and geometry update is introduced. User may choose either linear (1 iteration) or non-linear analysis (multiple iterations). Further information about the non-linear procedure is given in section 3.3.3.

3.2.6 Output setting

KuFEM exports number of spreadsheet tables after the calculation is successfully finished. In order to help the user with the post-processing, the delimiters can be adjusted. This should avoid any potential problem user might face with his computer setting.

3.3 Analysis work-flow and equations

Principle, how KuFEM calculates the analysis is shown on diagram 3.7. Firstly, the geometry data processing is explained. Next section describes displacement vector determination. Other sections are focused on forces, stresses and strains calculation.

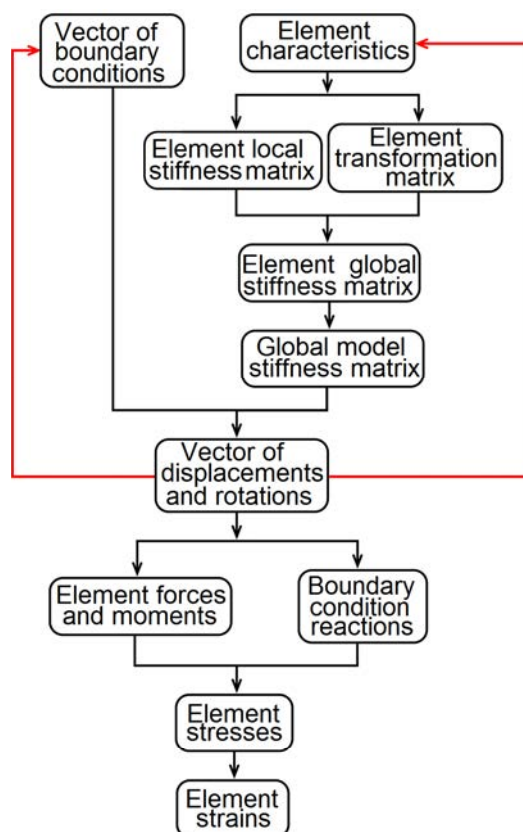


Figure 3.7: Diagram of calculation algorithm including non-linear procedure (red lines).

3.3.1 Geometry data processing

At this point, user has successfully loaded the geometry, element properties and filled out the boundary conditions. After pressing on *Run calculation* button, the data input is processed by determining the number of degrees of freedom:

$$no_{DOF} = 3 \cdot no_{Nod} \quad (2)$$

All elements are defined through the upper and lower flange (thickness and elastic modulus). However the mathematical formulation of beam elements does not accept this definition. For this purpose an effective properties will be calculated. This effective elastic modulus serve as a reference value to which the properties are transformed.

- element effective elastic modulus:

$$E_{EFi} = \frac{t_{Hi} \cdot E_{Hi} + t_{Di} \cdot E_{Di}}{t_{Hi} + t_{Di}} \quad (3)$$

First parameter of the element is the cross-section area, perpendicular to the mid-fibre:

- cross-section area:

$$A_i = t_{Hi} \cdot B_i \cdot \frac{E_{EFi}}{E_{Hi}} + t_{Di} \cdot B_i \cdot \frac{E_{EFi}}{E_{Di}} \quad (4)$$

Next step is to calculate the position of neutral axis. Neutral axis (figure 3.8) is determined from the total thickness of the element and from the thickness and stiffness of the flanges.

$$NO_i = \frac{1}{2} \cdot t_{Di} + t_{Hi} \cdot E_{Hi} \cdot \frac{T_i - \frac{1}{2} \cdot (t_{Di} + t_{Hi})}{t_{Di} \cdot E_{Di} + t_{Hi} \cdot E_{Hi}} \quad (5)$$

The 2nd moment of area of the element cross-section needs to be calculated. It is calculated as a sum of upper and lower flange moment of area. Upper flange moment is denoted as JJ_{Hi} whereas the lower flange moment is denoted as JJ_{Di} .

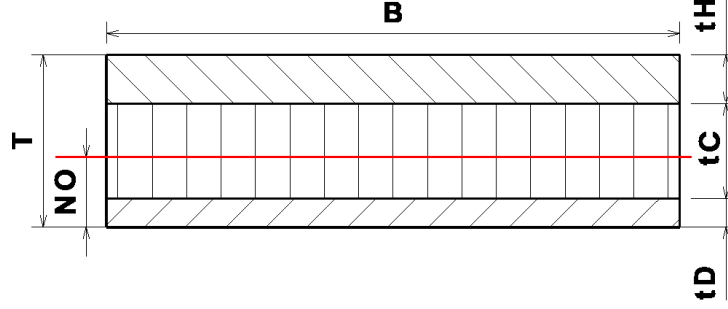


Figure 3.8: Neutral axis of a cross-section.

- 2nd moment of area, upper flange to neutral axis:

$$JJ_{Hi} = \frac{1}{12} \cdot \left(B_i \cdot \frac{E_{EFi}}{E_{Hi}} \right) \cdot t_{Hi}^3 + \left(B_i \cdot \frac{E_{EFi}}{E_{Hi}} \right) \cdot t_{Hi} \cdot \left(T_i - NO_i - \frac{1}{2} \cdot t_{Hi} \right)^2 \quad (6)$$

- 2nd moment of area, lower flange to neutral axis:

$$JJ_{Di} = \frac{1}{12} \cdot \left(B_i \cdot \frac{E_{EFi}}{E_{Di}} \right) \cdot t_{Di}^3 + \left(B_i \cdot \frac{E_{EFi}}{E_{Di}} \right) \cdot t_{Di} \cdot \left(NO_i - \frac{1}{2} \cdot t_{Di} \right)^2 \quad (7)$$

- total 2nd moment of area to lateral axis:

$$JJ_i = JJ_{Hi} + JJ_{Di} \quad (8)$$

- 2nd moment of area to through-thickness axis:

$$JK_i = \frac{1}{12} \cdot \left(B_i \cdot \frac{E_{EFi}}{E_{Hi}} \right)^3 \cdot t_{Hi} + \frac{1}{12} \cdot \left(B_i \cdot \frac{E_{EFi}}{E_{Di}} \right)^3 \cdot t_{Di} \quad (9)$$

Now only the geometrical parameters length and angle are calculated:

- length of an element is calculated from node coordinates:

$$L_i = \sqrt{(Y_i - Y_{i+1})^2 + (Z_i - Z_{i+1})^2} \quad (10)$$

- sinus value:

$$\sin_i = \frac{Z_{i+1} - Z_i}{L_i} \quad (11)$$

- cosin value:

$$\cos_i = \frac{Y_{i+1} - Y_i}{L_i} \quad (12)$$

At this point the stiffness matrix and transformation matrix of each element can be formulated.

3.3.2 Deformation

This calculation is based on an assumption, that the X-direction displacement is not significant in comparison to the Y and Z directions. Assuming $UX = 0$ significantly reduces difficulty of the problem. Only two translations and one rotation for each node will be calculated (see figure 3.9).

Either Timoshenko or Euler-Bernoulli beam theory can be chosen. The difference is the element stiffness matrix. Equation 13 shows the LS matrix for Timoshenko beam. By giving $\Phi = 0$ the matrix is reduced to the Euler-Bernoulli theory. The parameter Φ gives the relative importance of the shear deformations to the bending deformations.

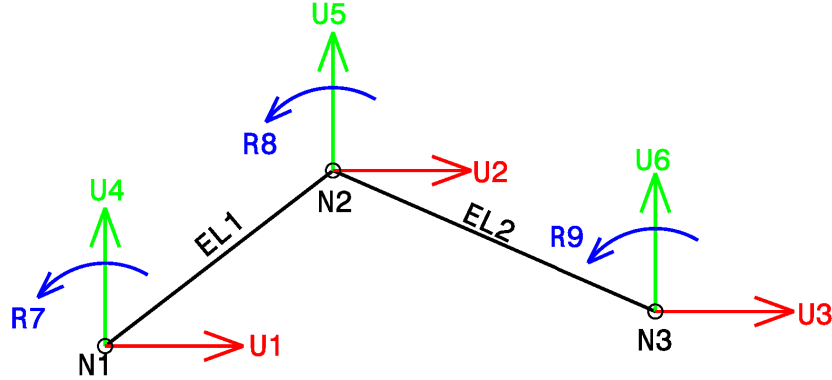


Figure 3.9: Degrees of freedom numbering (U=translation, R=rotation, N=node and EL=element).

Local stiffness matrix is calculated for each element³⁴:

$$[LS] = \begin{bmatrix} \frac{A \cdot E}{L} & -\frac{A \cdot E}{L} & 0 & 0 & 0 & 0 \\ -\frac{A \cdot E}{L} & \frac{A \cdot E}{L} & 0 & 0 & 0 & 0 \\ 0 & 0 & \frac{12}{1+\Phi} \cdot \frac{E \cdot JJ}{L^3} & \frac{-12}{1+\Phi} \cdot \frac{E \cdot JJ}{L^3} & \frac{6}{1+\Phi} \cdot \frac{E \cdot JJ}{L^2} & \frac{6}{1+\Phi} \cdot \frac{E \cdot JJ}{L^2} \\ 0 & 0 & \frac{-12}{1+\Phi} \cdot \frac{E \cdot JJ}{L^3} & \frac{12}{1+\Phi} \cdot \frac{E \cdot JJ}{L^3} & \frac{-6}{1+\Phi} \cdot \frac{E \cdot JJ}{L^2} & \frac{-6}{1+\Phi} \cdot \frac{E \cdot JJ}{L^2} \\ 0 & 0 & \frac{6}{1+\Phi} \cdot \frac{E \cdot JJ}{L^2} & \frac{-6}{1+\Phi} \cdot \frac{E \cdot JJ}{L^2} & \frac{4+\Phi}{1+\Phi} \cdot \frac{E \cdot JJ}{L} & \frac{2-\Phi}{1+\Phi} \cdot \frac{E \cdot JJ}{L} \\ 0 & 0 & \frac{6}{1+\Phi} \cdot \frac{E \cdot JJ}{L^2} & \frac{-6}{1+\Phi} \cdot \frac{E \cdot JJ}{L^2} & \frac{2-\Phi}{1+\Phi} \cdot \frac{E \cdot JJ}{L} & \frac{4+\Phi}{1+\Phi} \cdot \frac{E \cdot JJ}{L} \end{bmatrix} \quad (13)$$

Each element is positioned at a different angle, relative to the YZ axis. In the next step a transformation matrix of goniometric functions is calculated:

$$[T] = \begin{bmatrix} \cos_i & 0 & \sin_i & 0 & 0 & 0 \\ 0 & \cos_i & 0 & \sin_i & 0 & 0 \\ -\sin_i & 0 & \cos_i & 0 & 0 & 0 \\ 0 & -\sin_i & 0 & \cos_i & 0 & 0 \\ 0 & 0 & 0 & 0 & 1 & 0 \\ 0 & 0 & 0 & 0 & 0 & 1 \end{bmatrix} \quad (14)$$

³The lower index 'i' is omitted for the sake of clarity.

⁴The elastic modulus of the element is marked as 'E', however the effective stiffness is used.

By multiplying these two matrices (T and LS) for each element a global stiffness matrix is obtained:

$$[GS_i] = [T_i]^{-1}[LS_i][T_i] \quad (15)$$

Combining all Global Stiffness matrices together creates Global Stiffness of the whole Model (GSM). This is ruled by the DOF number for each node.

$$[GSM] = \sum_{i=1}^{noEl} [GS_i] \quad (16)$$

Those DOF that were removed by boundary conditions are reflected in the GSM matrix and also in Loading Vector F. Final vector of displacements and rotations is obtained by multiplying the GSM matrix and Force vector:

$$\{U\} = [GSM] \{F\}^{-1} \quad (17)$$

Also the reactions can be determined by multiplying global stiffness matrix and transposed displacement vector:

$$\{R\} = [GSM] \cdot \{U\}^T \quad (18)$$

3.3.3 Geometrically non-linear analysis

Especially main landing gear is expected to achieve large deformations when dampening the landing shock force. Mr. Goyal emphasises the need for a non-linear analysis [22]. For this reason user can choose non-linear calculation by increasing the number of iterations.

Established procedure of non-linear analysis is based on Newton-Raphson technique. Each iteration involves formulation and solution of linearised equilibrium equations (updated stiffness matrix and solving the system).

Non-linear calculation reflects progressive deformation as a response to the increasing load. This is illustrated on figure 3.10 where linear and two-step non-linear calculation is illustrated. User may choose 5, 10 or 20 steps.

Diagram 3.7 illustrates the iteration loop by red lines.

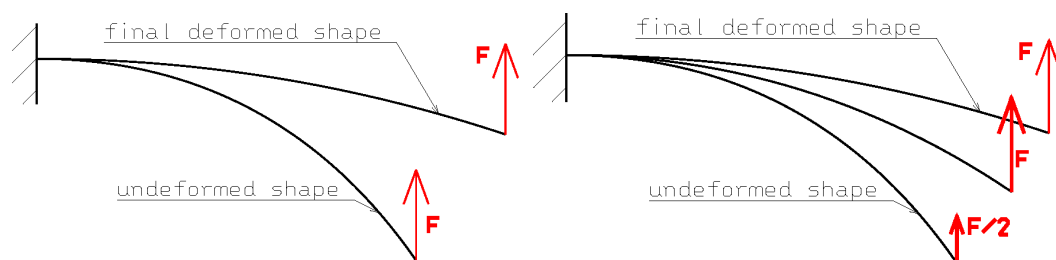


Figure 3.10: Difference between linear (1 step) and non-linear (2 steps) calculation.

3.3.4 Forces and Moments distribution in global coordinate system

KuFEM offers three different types of boundary conditions. The forces and moments at the centre of each element must be calculated in accordance to these conditions.

Pinned BC

Loading is introduced at node L. At node A all degrees of freedom are removed (UY, UZ, RX). Figure 3.11 shows the influence lines.

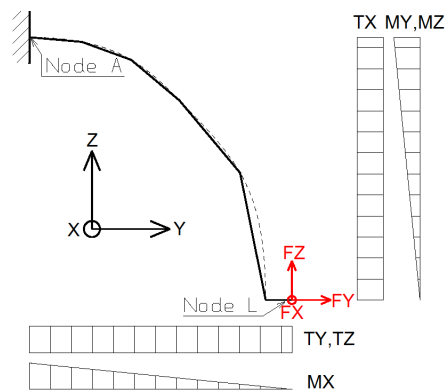


Figure 3.11: Influence lines for the pinned boundary condition.

Continuous BC

Loading is introduced at node L. At node A one rotation and one translation is removed (UY, RX). Node N removes the remaining degree of freedom (UZ). Figure 3.12 shows the influence lines.

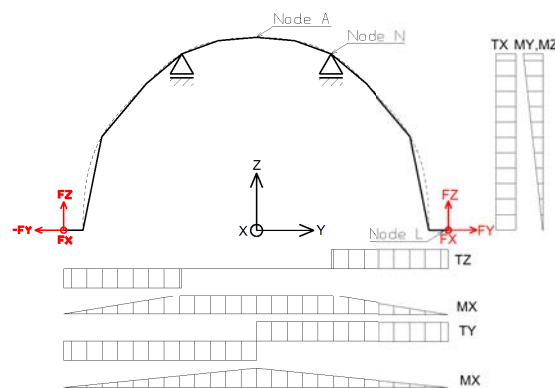


Figure 3.12: Influence lines for the continuous boundary condition.

Divided BC

Loading is introduced at node L. At node A two translations are removed (UY, UZ). Node A removes the remaining degree of freedom (UZ). Figure 3.13 shows the influence lines.

User should be aware of the fact, that the MX component caused from FY may not always be in correspondence with the actual geometry. However the described model ensures the calculation to be on a safe side.

3.3.5 Forces and Moments on Element

The forces and moments in global coordinate system are calculated at the centre of each element (figure 3.14). These forces and moments are transformed into the local element coordinate system, unique to each element.

It has been described in previous section that the whole geometry is located in one plane; therefore the geometry is two dimensional. An angle between the element longitudinal axis \vec{l} and global horizontal axis \vec{Y} can be calculated. According to this angle (figure 3.14) all forces and moments are transformed into the element coordinate system.

- characteristic angle is also calculated from node coordinates:

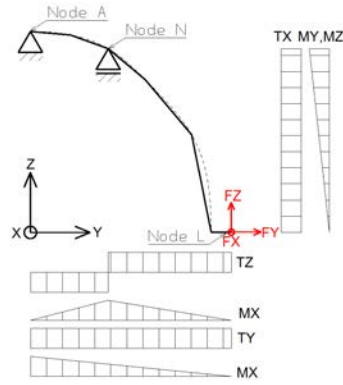
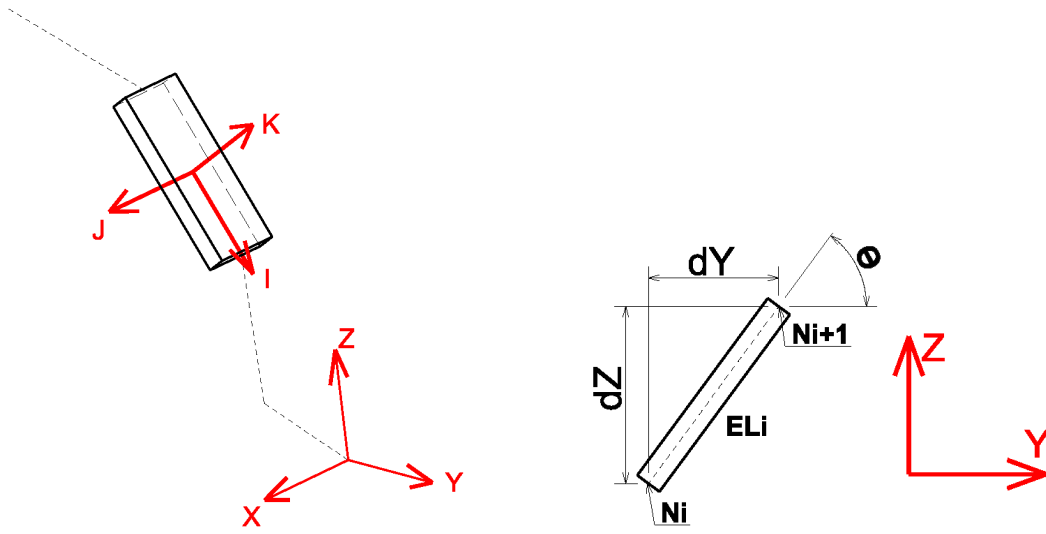


Figure 3.13: Influence lines for the divided boundary condition.

Figure 3.14: Element geometry and loading (left). Characteristic angle θ (right).

$$\theta_i = \arctan\left(\frac{dZ}{dY}\right) = \arctan\left(\frac{Z_{i+1} - Z_i}{Y_{i+1} - Y_i}\right) \quad (19)$$

- element longitudinal force is calculated from element centre coordinates:

$$FI_i = FY_i \cdot \cos(\theta_i) + FZ_i \cdot \sin(\theta_i) \quad (20)$$

- element lateral force does not change:

$$FJ_i = FX_i \quad (21)$$

- element through-thickness force:

$$FK_i = FZ_i \cdot \cos(\theta_i) - FY_i \cdot \sin(\theta_i) \quad (22)$$

- element twisting moment:

$$MI_i = MY_i \cdot \cos(\theta_i) + MZ_i \cdot \sin(\theta_i) \quad (23)$$

- element lateral bending moment

$$MJ_i = MX_i \quad (24)$$

- element bending moment:

$$MK_i = MZ_i \cdot \cos(\theta_i) - MY_i \cdot \sin(\theta_i) \quad (25)$$

3.3.6 Stress analysis

General FEM approach to determine stresses and strains is to solve strains through strain-displacement matrix and than obtain the stresses by multiplying the strain vector by stiffness matrix:

$$\begin{aligned}\{\epsilon\} &= [B] \{u\} \\ \{\sigma\} &= [GSM] \{\epsilon\}\end{aligned}$$

Where the matrix $[B]$ is the strain displacement matrix. It represents a function of the partial derivatives of shape functions with respect to the global XYZ coordinate system. This leads to Jacobian introduction. Jacobian matrix relates derivatives of the function in local coordinate system to derivatives in global coordinate system.

For KuFEM this approach will be substituted by more intuitive approach, based on geometry and already known element forces. Another advantage of suggested approach is that it is not limited by planar definition of the displacement calculation described above. Suggested approach follows simple idea, familiar to all engineering students:

$$\frac{Force}{Area} \rightarrow Stress \quad \text{and} \quad \frac{Stress}{Stiffness} \rightarrow Strain$$

Another advantage of this approach uses the element definition from section 3.2.1. This element definition allows to account for unsymmetrical flanges (geometry and material). Method is based on [8].

Each element is loaded by three forces and three moments. These forces and moments were determined in previous sections. At this point, stresses are going to be calculated. Four locations in the cross-section are picked as the most loaded points. These points are denoted as C, D, E and F. In rectangular cross-section these points are the vertexes as shown on figure 3.15. These points are equivalent to NASTRAN solutions. [3, 3049-3056]. Dimensions are defined on figures 3.6. Figure 3.16 shows the cross-section stress loading by given force or moment, whereas figure 3.17 shows the shear flow in the wrap.

The following stresses are calculated for the flanges:

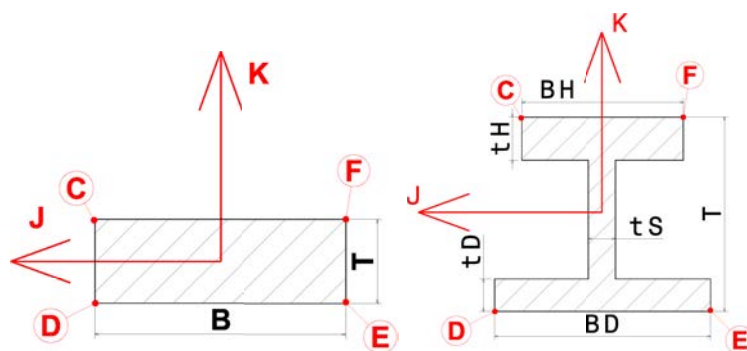


Figure 3.15: Cross-section points for stress calculation. Rectangular and I cross-section.

- normal tensile/compression⁵ stress:

$$\sigma_{I_i} = \frac{F I_i}{B_i \cdot (t_{H_i} + t_{D_i})} \quad (26)$$

- bending stress at CF edge⁶:

$$\sigma_{J_{CF_i}} = \frac{M J_i}{J J_i} \cdot (T_i - N O_i) \quad (27)$$

- bending stress at DE edge:

⁵Tensile / compression stress component does not require recalculation due to different elastic modulus, because of the assumption that both flanges are made from the same material and both are loaded in the same direction.

⁶Different tensile / compression module is incorporated into the Neutral axis position NO .

$$\sigma_{J_{DEi}} = \frac{MJ_i}{JJ_i} \cdot NO_i \quad (28)$$

- bending stress due to MK ⁷:

$$\sigma_{K_i} = \frac{MK_i}{JK_i} \cdot \frac{1}{2} \cdot B_i \quad (29)$$

- total stress at point C:

$$\sigma_{C_i} = \sigma_{I_i} + \sigma_{J_{CFi}} + \sigma_{K_i} \quad (30)$$

- total stress at point D:

$$\sigma_{D_i} = \sigma_{I_i} + \sigma_{J_{DEi}} - \sigma_{K_i} \quad (31)$$

- total stress at point E:

$$\sigma_{E_i} = \sigma_{I_i} - \sigma_{J_{DEi}} - \sigma_{K_i} \quad (32)$$

- total stress at point F:

$$\sigma_{F_i} = \sigma_{I_i} - \sigma_{J_{CFi}} + \sigma_{K_i} \quad (33)$$

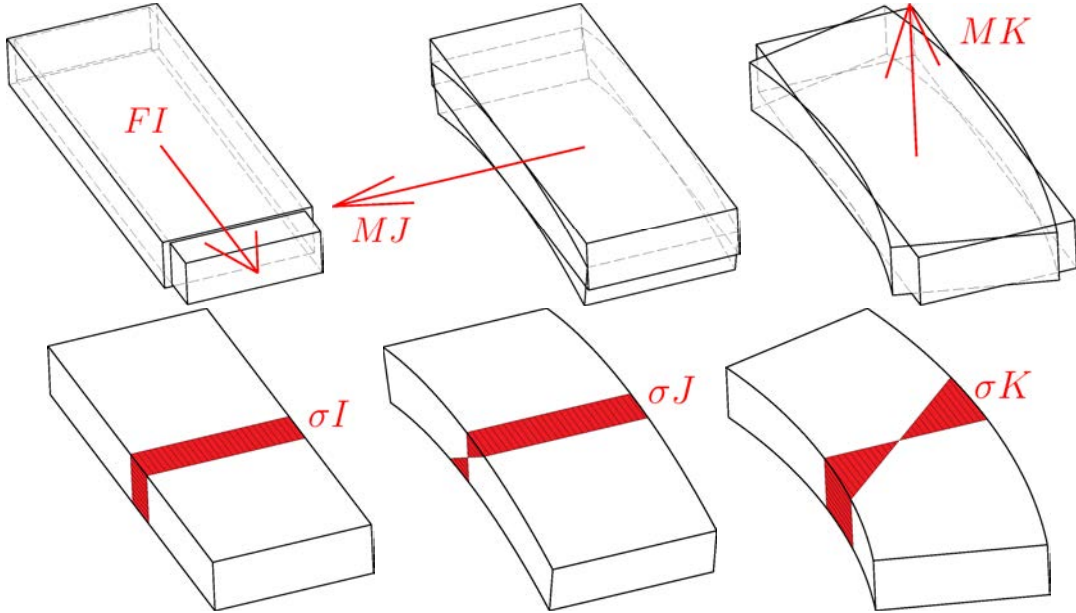


Figure 3.16: Force FI causes stress σ_I . Moment MJ causes stress σ_J . Moment MK causes stress σ_K .

Standard beam elements do not support stress and strain calculation in form required for the intended analysis. Following approach is applied.

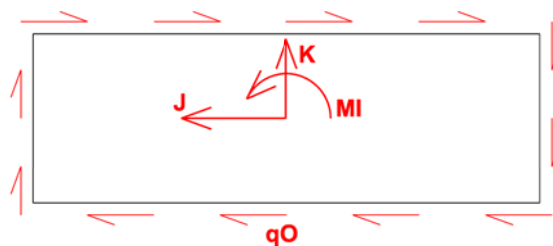
- shear flow from torsion:

$$q_{O_i} = \frac{MI_i}{2 \cdot T_i \cdot B_i} \quad (34)$$

- shear stress from torsion:

$$\tau_{O_i} = \frac{q_{O_i}}{t_{O_i}} \quad (35)$$

⁷Tensile / compression stress component does not require recalculation due to different elastic modulus, because of the symmetrical arrangement of the flanges.

Figure 3.17: Moment MI causes stress τ_O .

3.3.7 Normal stress through thickness

When using the divided or continuous boundary condition, important problem is the through-thickness stress in the area of the outer hinge. For this reason is user required to input the attachment width R . Width B is an average value between the two neighbouring elements.

- through-thickness stress:

$$\sigma_{TT} = \frac{2}{R \cdot (B_{N-1} + B_N)} \cdot F_Z \cdot \frac{Y_L - Y_N}{Y_N - Y_1} \quad (36)$$

3.3.8 Shear stress through thickness

This section has been developed as a part of KuFEM's later versions. Therefore new definitions are necessary in order to describe the calculation of the shear stress through thickness (figure 3.18).

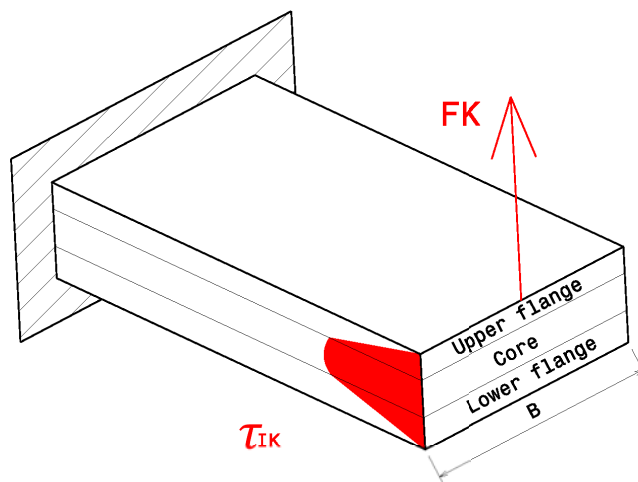


Figure 3.18: Shear stress through thickness of the element.

Shear stress through thickness is based on [12], a simplified method introduced by Mr. Bednarczyk in 2008.

In general, the calculation expects the cross-section to consist of three plies: upper and lower flange and the core. Each cross-section constituent has its own stiffness modulus.

Since the KuFEM is now focussing also on the core a change in the input data seemed reasonable. Original input set of data describing the thickness was T , t_H and t_D (section 3.2.1). Now it has been changed to more logical t_H , t_C and t_D . Each constituent is also described by its stiffness: E_H , E_C and E_D .

First the basic parameters are determined:

- Total thickness:

$$T = t_H + t_C + t_D \quad (37)$$

- Effective stiffness (upgraded equation 3):

$$E_{EF} = \frac{t_H \cdot E_H + t_C \cdot E_C + t_D \cdot E_D}{T} \quad (38)$$

- Neutral axis position (upgraded equation 5):

$$NO = \frac{1}{T \cdot E_{EF}} \cdot \left[\frac{1}{2} \cdot E_D \cdot t_D^2 + t_C \cdot E_C \cdot \left(t_D + \frac{1}{2} \cdot t_C \right) + t_H \cdot E_H \cdot \left(t_D + t_C + \frac{1}{2} \cdot t_H \right) \right] \quad (39)$$

The shear flow through the thickness is calculated from the width of the element.

- Shear flow:

$$q_{IK} = \frac{F_K}{B} \quad (40)$$

Further equations determine the 2nd moment of area of the cross-section:

- Upper flange: see equation 6.
- Lower flange: see equation 7.
- Core:

$$JJ_C = B \cdot \frac{E_{EF}}{E_C} \cdot t_D \cdot \left[\frac{1}{12} \cdot t_C^2 + \left(NO - \frac{1}{2} \cdot t_C - t_D \right)^2 \right] \quad (41)$$

- Total (upgraded equation 8):

$$JJ = JJ_H + JJ_C + JJ_D \quad (42)$$

Next objective is to divide the cross-section into several slices⁸ (figure 3.19) and calculate the first moment of area:

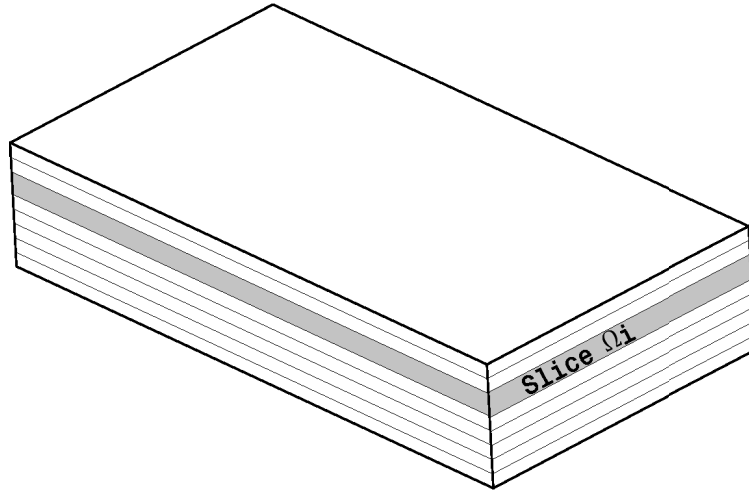


Figure 3.19: Element has been divided to several slices in through-thickness direction.

- Slice addition to the first moment of area:

$$\Delta S_{\Omega_i} = \frac{1}{2} \cdot B \cdot \frac{E_C}{E_{EF}} \cdot (k_i^2 - k_{i+1}^2) \quad (43)$$

- First moment of area at K:

$$S_K = \sum_{k=-NO}^{k=K} \Delta S_{\Omega} \quad (44)$$

And finally the distribution of the shear stress through thickness can be calculated:

- Shear stress distribution on a cross-section:

$$\tau_{IK} = \frac{q_K}{JJ} \cdot S_K \quad (45)$$

The resulting shear stress distribution may look similar to figure 3.20.

⁸KuFEM pre-set value is 50 slices regardless the total thickness T .

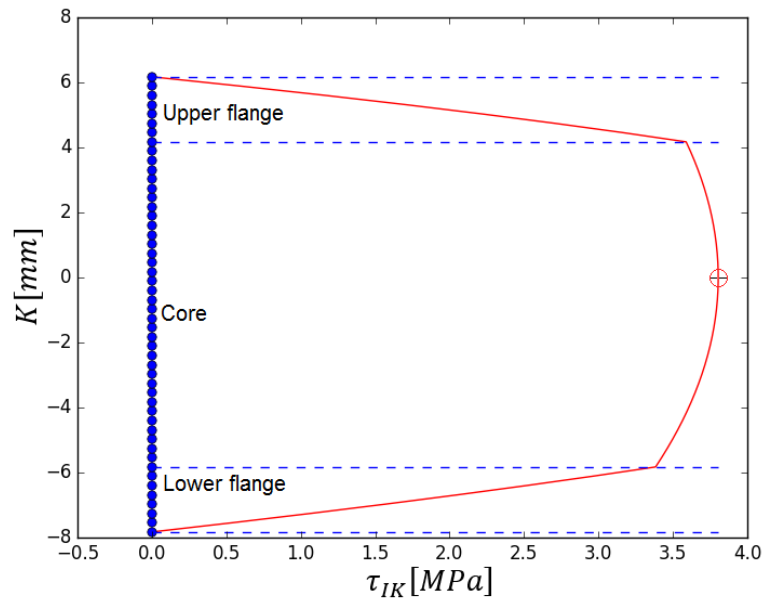


Figure 3.20: Typical distribution of shear stress on a cross-section made out of two flanges and core.

KuFEM output of this calculation for each element is only the maximum shear stress and it's position.

3.3.9 Strain analysis

Having determined the normal stresses at points C,D,E and F, now the simplified Hook's law is used to determine the actual strain:

$$\epsilon_{ji} = 100 \cdot \frac{\sigma_{ji}}{E_{ji}} \quad (46)$$

where the index i denotes the number of element and index j denotes the location in the element. In this manner the difference between compression and tensile modulus is taken into account. The strain is given in [%] for user comfort. For example typical fibre glass, used for structural parts, is to withstand about 3.5% of strain [28] before destruction. This gives fast and easy reference how well the material's potential is used.

3.4 Output functions

A useful function is to export the deformed geometry in order to evaluate potential collisions with surrounding structure. KuFEM allows to export an IGES file, which is universal and contains the deformed geometry.

Other output function allow user to generate an input file for commercial solvers (NASTRAN and Abaqus).

4 Practical examples of KuFEM results

4.1 HPH Shark Composite Wing

The wing segment, which has been tested at the IAE, is the root section of a full composite wing. Tested segments were not equipped with flaps. Structurally the segments were identical to the wing: main spar made out of a foam core and thick carbon flanges.

The first five specimens were subjected to static tests, on the other four specimens fatigue tests were conducted. Static tests of two whole wings were also carried out. The figure 4.1 shows the fatigue test layout of X06 specimen in 2007.



Figure 4.1: Layout of X06 wing segment fatigue test. Archive of IAE.

Parts of this chapter were published as papers [31] under the title *"Modifications of a simple I-beam and its Effects on the Stress State"* and in [30] as *"Stress-deformation analysis of a composite wing segment"*. The first article has investigated the changes in stresses according to the structure shape and boundary conditions. The other describes simulation of the static wing segment test.

The author has also published an article about acoustic emission as a monitoring method used during the fatigue test of these segments. The article is entitled *"Acoustic Emission Localization in Testing of Composite Structures"* [32].

Three different programs are used to analyse the wing segment. First prediction is obtained from KuFEM (Euler-Bernoulli and Timoshenko, linear and non-linear prediction), then a NAS-TRAN finite element analysis (1D and 2D analysis), and a quick deformation analysis made in Ministatik. In the summary the deflection, strains and element forces are compared.

4.1.1 Loading

The original geometry and loading has been reduced. Geometrical changes include the removal of skin, rib and rear spar. Loading has reduced the forces (no counter F_Z force in the root rib) and twisting moment at the tip. Boundary conditions changed also. Original boundary conditions are shown on figure 4.2 (left), whereas the reduced boundary conditions are shown on figure 4.2 right). This simplified geometry, loading and boundary conditions will be used in analysis presented here after.

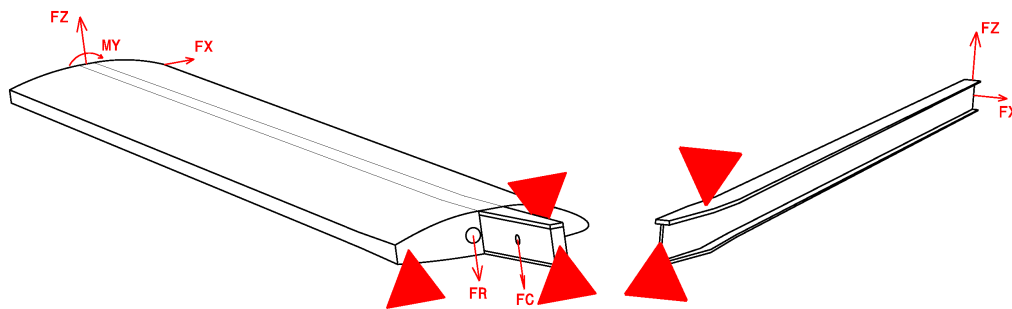


Figure 4.2: Left: original loading of the wing segment. Right: simplified model for verification analysis.

Displacement vectors were calculated by three different methods. Firstly in KuFEM. From KuFEM a BDF file has been generated and analysed by NASTRAN. Another NASTRAN analysis using shell elements has been adopted from [31]. For third independent prediction Ministatik has been used.

4.1.2 Results

Deflection

Not only the last node displacement is important. The displacement along the wing span are also important. Following figures 4.3 and 4.4 shows the UZ span-wise displacement function. A special emphasis is given to the linear and non-linear calculation.

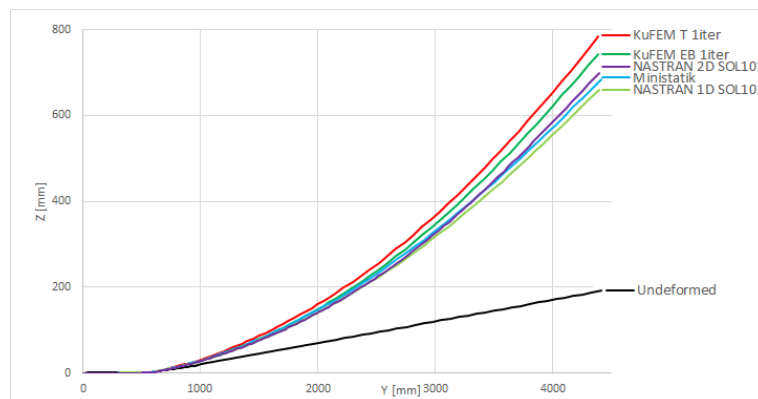


Figure 4.3: Deformed mid-fibre comparison for linear (1 iteration) solutions.

Strains

Strains are compared only for linear solutions. Figure 4.5 show the strains of KuFEM Euler-Bernoulli 1 iteration solution, KuFEM Timoshenko 1 iteration solution, NASTRAN 1D and 2D SOL101 solutions.

4.1.3 Summary

Three analysis of a wing segment are presented (KuFEM, NASTRAN and Ministatik). Further more different models and different theories are used. Total of 10 different variants are shown and discussed. The results are compared in terms of displacement and strains.

Comparison of strains on figures 4.3 and 4.4 shows good agreement between all analysis variants. Even more so, the comparison confirmed the claims of [7] that Euler-Bernoulli beam

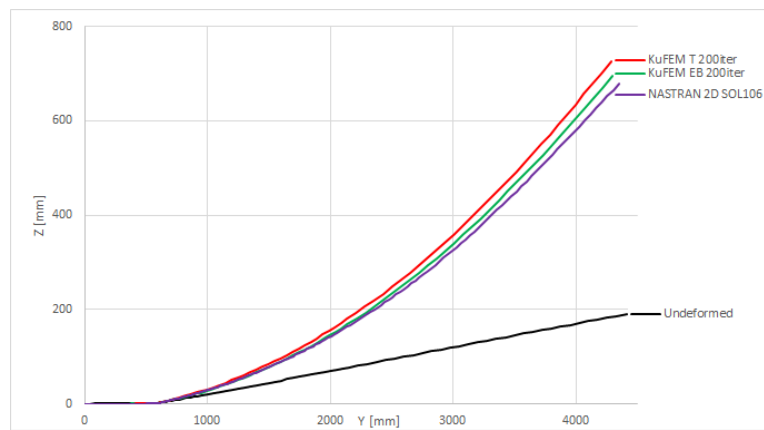


Figure 4.4: Deformed mid-fibre comparison for non-linear (multiple iterations) solutions.

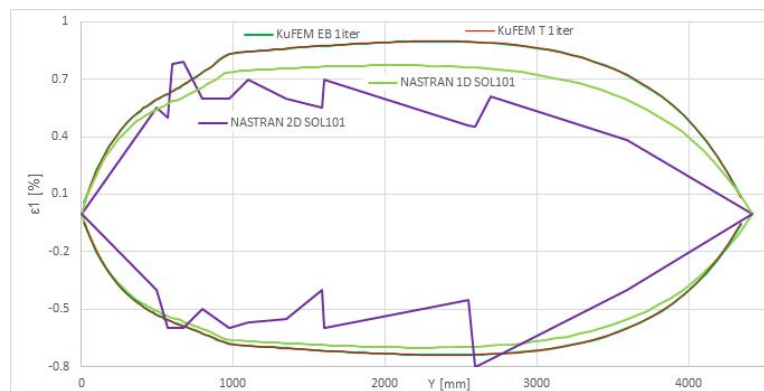


Figure 4.5: Strains in the longitudinal element direction.

formulation is stiffer than Timoshenko formulation.

A search to lower the work load in modelling the 2D model took its toll in the strain results (figure 4.5). Not only is the distribution scarred by steps, but also the effect of changing slope is traceable. Also interesting observation is that the 2D model is stiffer as a result of the method used to replace the real flange thickness distribution.

4.2 Main Landing Gear Spring of Merlin 103

Merlin 103 is an UL-category airplane with tricycle landing gear. Main landing gear is made of a single composite spring lags, attached at each side of the fuselage. This type of attachment is called continuous (see figure 3.12).

4.2.1 Models for Verification

For the KuFEM calculation to be verified, two other models are devised. First, the KuFEM-generated 1D NASTRAN model. Then another NASTRAN model, that uses 2D shell elements. This NASTRAN 2D model will allow to use non-linear solver SOL 106.

4.2.2 Results

Total of 6 calculations were made. Three KuFEM, using linear and non-linear formulation, and linear NASTRAN analysis with 1D elements and finally NASTRAN model with shell elements using linear and non-linear solvers:

- KuFEM: linear
- KuFEM: non-linear, 10 iterations
- KuFEM: non-linear, 100 iterations
- NASTRAN 1D: linear
- NASTRAN 2D: linear
- NASTRAN 2D: non-linear, 10 iterations

Deflection

Figure 4.6 shows a front view of the landing gear. There is shown the initial un-deformed geometry (black). In green a deformed 2D NASTRAN linear solution is shown. And finally in red the linear KuFEM and NASTRAN beam deformed geometries are presented.

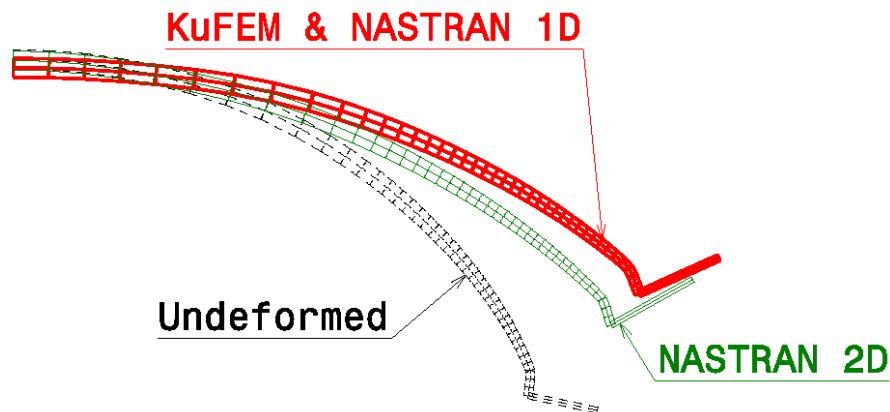


Figure 4.6: Comparison of deformed shapes obtained from KuFEM and NASTRAN (both 1D and 2D).

Results: Strains

Presented strains (figure 4.7) are measured in the element longitudinal axis - ϵ_I for KuFEM and NASTRAN 1D results. The results of NASTRAN 2D model are presented as the major and minor strains.

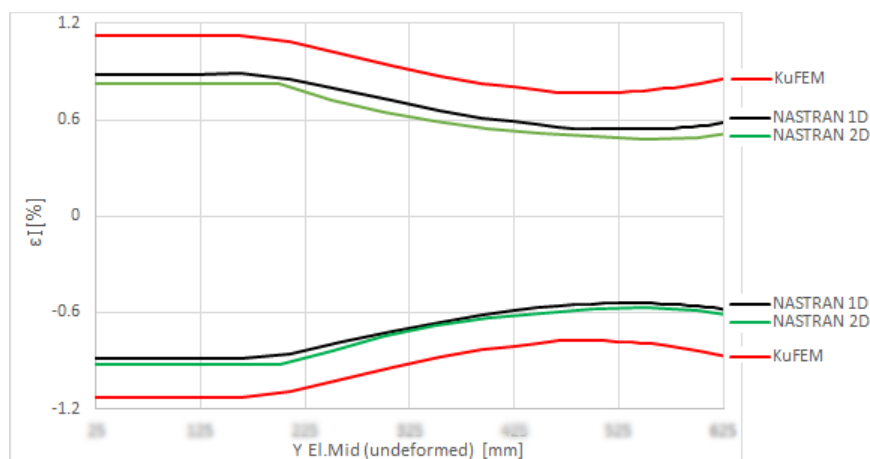


Figure 4.7: Comparison of ϵ_1 strains obtained from KuFEM and NASTRAN.

Strains, predicted by KuFEM are higher than the NASTRAN prediction. At the fuselage attachment, the strain predicted by KuFEM is $\epsilon_{KuFEM} = 1.1\%$. At the same location, the

NASTRAN beam model predicts $\epsilon_{NASTRAN} = 0.875\%$. From here, the ratio is:

$$k = \frac{\epsilon_{KuFEM}}{\epsilon_{NASTRAN}} = \frac{1.1}{0.875} = 1.257$$

This difference is largely attributed to the fact, that KuFEM calculates it's stresses and strains using deformed geometry, while NASTRAN uses the geometry un-deformed. The presented strains are caused by the bending moment MX , which is mainly caused by the vertical force RF_Z at a distance ΔY . The difference in ΔY of deformed versus un-deformed geometry creates the difference (figure 4.8). In this case, the ratio is:

$$k = \frac{MX_{deformed}}{MX_{undeformed}} = \frac{\Delta Y_D}{\Delta Y_U} = 1.276$$

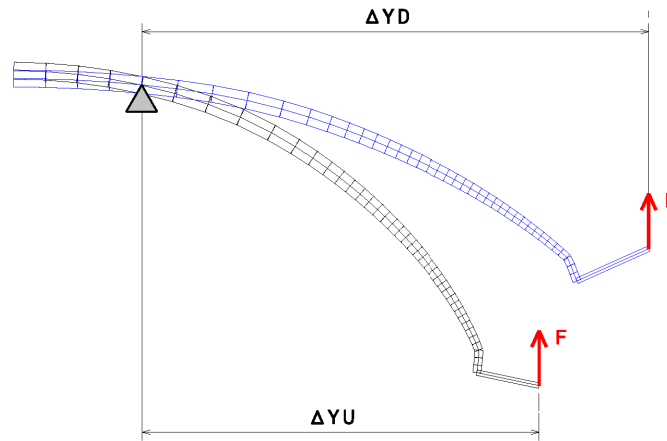


Figure 4.8: Different position of the vertical force.

4.2.3 Summary

Presented results provided good accuracy in deflection (within 5.9% in single iteration and 2.1% in multiple iteration loop). More interesting is the comparison in strain values between NASTRAN linear solution and KuFEM solution. As the NASTRAN SOL 101 solver determines the strains on un-deformed geometry, the results are less accurate compared to the KuFEM.

4.3 Nose Wheel Spring of Merlin 103

The spring is located on the nose wheel (figure 4.9), connecting lower tube with upper assembly. The most severe loading is caused by horizontal landing. This loading is compressing the nose gear and the spring is loaded by bending momentum and shear force.



Figure 4.9: Nose gear spring on the airplane.

4.3.1 Numerical predictions

KuFEM Analysis

From volume fraction the local stiffness modulus for each element (as an average between each node) has been determined. Both limit and ultimate load has been calculated with linear and 10-iterations non-linear solving methods. Figure 4.10 shows the working diagram calculated by KuFEM.

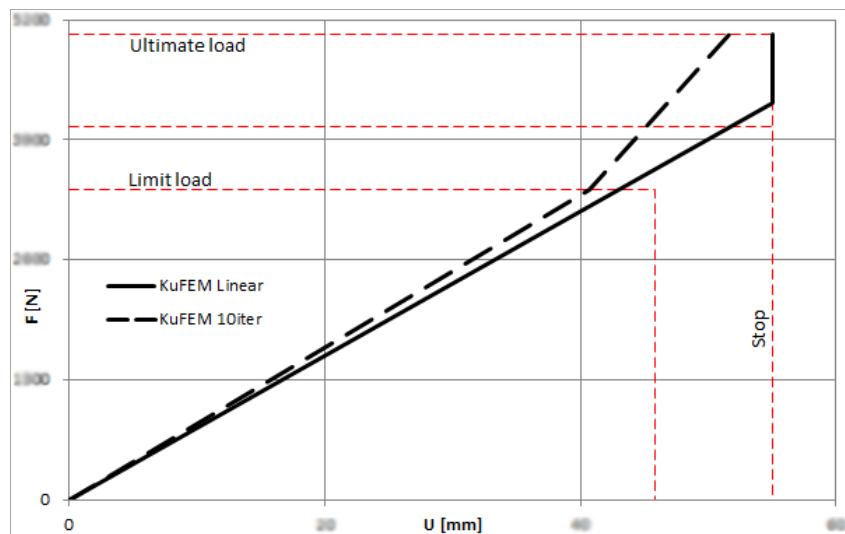


Figure 4.10: Working diagram as predicted by KuFEM models.

NASTRAN Analysis

In order to validate the KuFEM results, another analysis used MSC.Patran/NASTRAN software. First analysis used the BDF file generated by KuFEM with beam elements (figure 4.11, left). The other used 8-node HEX 3D element (figure 4.11, right) based on suggestions from [11]. Both simulations used linear SOL101 solver. Further non-linear SOL106 solver has been used for the CHEXA model.

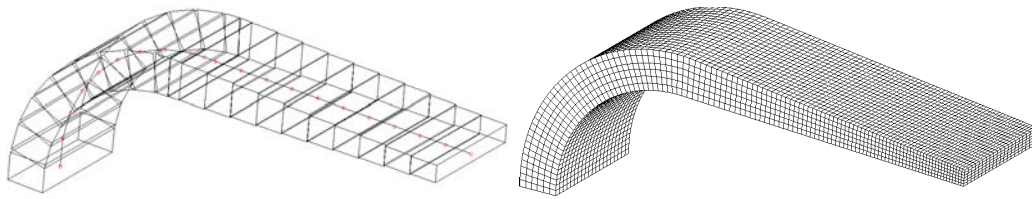


Figure 4.11: NASTRAN finite element model generated from KuFEM BDF file (left) and model made of 3D CHEXA elements (right).

4.3.2 Lab Tests

First three springs produced were tested in the laboratory (figure 4.12) in order to verify the calculation and establish the manufacturing variance. Each sample had been measured several times close to or slightly above the limit load.

All measured values suggest linear behaviour (diagram 4.13, grey area) in the measured range.



Figure 4.12: Spring in the test jig with control marks.

4.3.3 Summary

A nose gear spring was designed using KuFEM software. The task was to design a spring for given loading and travel distance. The required working diagram is shown on figure 4.13 in red dashed lines. Same problem has been analysed in MSC.Patran/NASTRAN with beam and CHEX elements.

When first specimens were available the laboratory tests took place. Total of 9 measurements on three specimens were made. Evaluation of these tests created an interval of working diagram. Figure 4.13 compares the best results obtained from KuFEM and NASTRAN in correlation with the lab results.

Linear solution fits the reality the best in both solutions. KuFEM beam model gives the best fit - right in the middle of the interval measured in the lab tests. NASTRAN CHEXA model gives stiffer results.

Very important factor is the manufacturing method, which uses a precise NC machined pressure moulds. Also the layup is simple (no core or cavities). Another factor is the workmanship (manufacturer has a long years of experience and follows the drawing instructions).

The stops were reached during the tests. No failure has occurred whatsoever. The spring is safe to operate. However no failure data were produced and stress/strain evaluation has not been done.

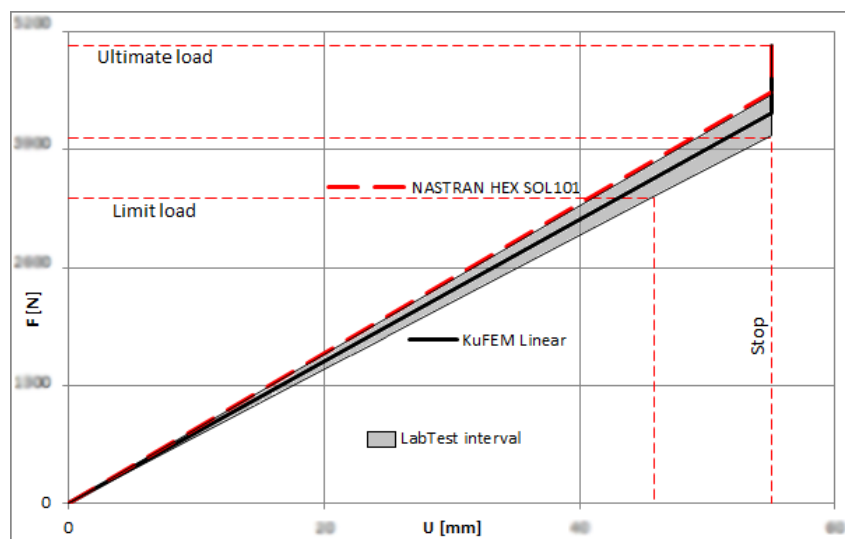


Figure 4.13: Final comparison of the KuFEM, NASTRAN and lab test results.

4.4 Tail Gear Spring of Merlin 110

With development of Merlin's tail gear variant a need to design a composite spring emerged. It has been decided to use glass UD fibres, the same as in nose gear spring (chapter 4.3). Except this time there will be also additional layers of $\pm 45^\circ$ fabric.

4.4.1 Laboratory test

All the described loadings were tested up to the ultimate load. No destruction of the composite has occurred. Therefore no relevant data on the failure were obtained.

Even though the worst loading case is the tail-down landing and the design has used this force, there is no laboratory data on the force / deflection relation because of the way the drop-tests are practised.

However adequate data were obtained during the supplementary up + aft test. For the purpose of evaluating the calculated results these data shall be used.

During the laboratory test a little over limit load is applied in the wheel axis at the defined angle. The displacement has been measured at the same place. Figure 4.14 shows the deformed shape of the tail gear.



Figure 4.14: Supplementary condition up + aft - limit load.

A contact between composite spring and the lower side of the fuselage is visible on figure 4.14. This effectively changes the boundary conditions from two supports to three (figure 4.15).

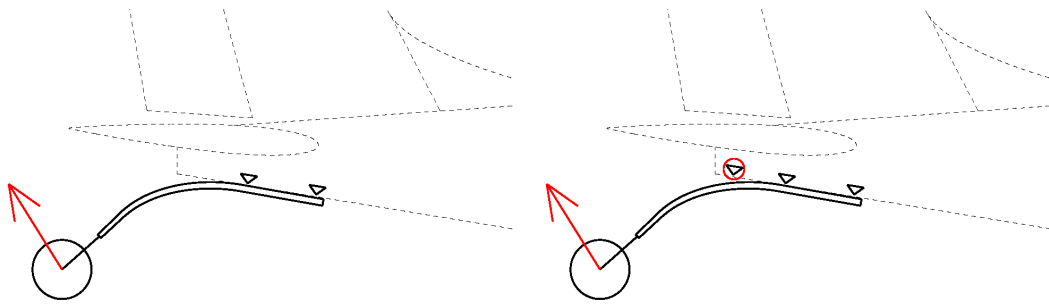


Figure 4.15: Change in boundary condition.

Contact between the tail and the tail gear's spring may not be a great deal in terms of certification, but it is a great deal in terms of predicted behaviour validity. The prediction does not have the ability to introduce additional support during the loading.

4.4.2 Comparison of Test and Prediction

The following analysis is by no means considered a valid proof and no firm conclusions may be taken from this. Only one measurement has been taken and the boundary condition of the test is inconsistent with the numerical analysis. However the comparison is presented to illustrate the difference.

Figure 4.16 shows similar deformed shape obtained from KuFEM and one measured during the limit load test. Worth noting is the fact, that while the real spring stopped upon contact with fuselage, the KuFEM did not have any additional boundary condition at this area and continued through the fuselage.

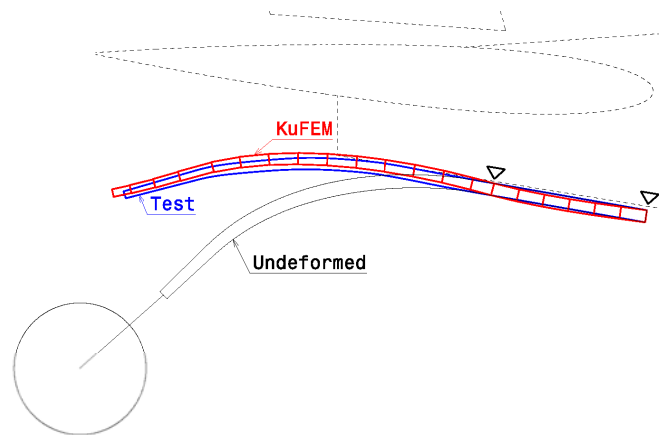


Figure 4.16: Comparison of deformed shapes, KuFEM vs. Limit load test.

5 Summary and Conclusion

5.1 Meeting the dissertation goals

Chapter 2.4 has set goals to be met in this dissertation thesis. Main goal was to develop a program, that would help in landing gear spring design. Using the program must be quick and simple with accurate results. The program is required to:

1. analyse typical thick composite parts,
2. predict displacements in one plane,
3. calculate the forces, moments, stresses and strains,
4. export results,
5. allow user to export deformed geometry,
6. allow user to export NASTRAN BDF file.

The inseparable part of KuFEM development is the verification and validation.

Chapter 3 describes the program operation: data input, deflection calculation, force and moment distribution, stress and strain calculation, geometry export and NASTRAN BDF file export functions. There are three verification examples showing the correlation to the closed-form solution of a simple-tension, simple-bending and simple-torque. Further verification and validation are shown in chapters 4.1, 4.2, 4.3 and 4.4.

First example in chapter 4.1 is based on HPH composite wing segment test. KuFEM results were compared to MiniStatik and NASTRAN solutions. Both, deflection and strains were compared. Difference between linear and non-linear solutions were also presented. All results are in excellent agreement and therefore the author considers KuFEM to be verified to produce correct results for this type of analysis.

The simplicity and flexibility of using KuFEM is presented in chapter 4.2. In the design process of a composite landing gear the iteration process is necessary, because the deflection influences the loading force. KuFEM linear and non-linear results are compared to the equivalent 1D and 2D NASTRAN models.

KuFEM analysis gives higher strains compared to NASTRAN (in this case approximately 25% higher). This is due to the fact, that KuFEM calculates the strains on deformed geometry (whereas the NASTRAN uses the un-deformed geometry). The difference is traced to the the arm of the bending moment, which is greater by 27% for the deformed geometry. These results are in agreement and therefore the author considers KuFEM to be verified to produce correct results for this type of analysis.

Different design approach is described in chapter 4.3. KuFEM is used to design the shape and layout of a nose wheel spring according to the required working diagram (force-displacement function). KuFEM is excellent help in this task, because it provides results immediately for the changes in geometry, stiffness and loading.

KuFEM results were verified with the NASTRAN 1D and 3D models. Laboratory tests were conducted on 3 specimens (total 9 measurements). The best results obtained from KuFEM and NASTRAN are from the linear analysis. KuFEM result is in excellent agreement with the measurement. The author considers KuFEM to be verified and validated (only deformation) to produce correct results for this type of analysis. Linear solution is preferred.

Similar design approach has been adopted for the tail gear spring, chapter 4.4. The laboratory test showed similar deflection of the spring as KuFEM did predict.

Spring touched the tail of the airplane during the test. This contact has changed boundary conditions. Therefore no reasonable data may be compared.

When the KuFEM deformed geometry of the spring has been compared with the tail of the airplane, similar clash has been detected. Because of this event KuFEM has been equipped with geometry output function. Now the user can easily export the deformed geometry. It can be inserted into the assembly and checked for clashes.

KuFEM has shown its flexibility, simplicity and usefulness in design of thick structural laminates, such as wing flanges and landing gear springs. The program has been verified and partially validated. Table 5.1 presents the verification and validation status:

KuFEM	Verification	Validation
Deflection	✓	✓
Stress and strains	✓	×

Table 5.1: KuFEM verification and validation status.

The goals, that were set in chapter 2.4, are fulfilled. The program for analysis of typical thick composite parts has been developed. It calculates loads, stresses and strains in the elements. Using KuFEM is easy and flexible. The results are exported and presented in understandable fashion. Among the results are universal geometry IGES files with un-deformed and deformed geometry and a BDF NASTRAN input file.

5.2 Contribution and novelty of the thesis

The outcome of this dissertation thesis is the development, verification and validation of KuFEM program. It is a simple-to-use program that combines in new original way following key elements:

1. established 2D finite element solution for beam deflection prediction,
2. simple force and moment equilibration in 3D,
3. Euler-Bernoulli and Timoshenko beam theory,
4. geometrically non-linear procedure,
5. composite oriented analysis,
6. 3D deformed geometry CAD output.

Among other FEA and stress analysis software, only KuFEM combines 2D deflection analysis and 3D stress components. Further more KuFEM introduces special element description in the stress analysis. This definition accounts for three different cross-section constituents and their specific material properties (upper and lower flange with core in between, each having its own elastic modulus). It has been verified, that using this formulation can increase accuracy of the beam deflection prediction to a full HEX NASTRAN model.

Useful KuFEM function is the possibility to export the task into NASTRAN and Abaqus input files (BDF and INP respectively).

Another unique function of KuFEM is the ability to export deformed CAD geometry (in universal IGES file), which can be used in clash analysis. This function is very uncommon even between first class commercial FEA software.

KuFEM program has found its place in TechProAviation company as a tool for analysis and manual optimization of thick composite structures (landing gears and springs). Program offers user-friendly interface, simple change in the geometry, property and loading.

5.3 Final conclusion

During the past seven years the author has participated on several projects at commercial and academic ground. These projects involved design, optimization, analysis and testing of aeronautical composite components. All these components resembled key similarities in terms of composite structure, manufacturing and loading. Namely these components are thick composite landing gear springs and wing spars.

In order to design, optimize and analyse these components, there were two different roads to go: either to use standard closed-form solution or exploit the hi-tech finite element software. Both options being extremely different with significant advantages and drawbacks. This state of affairs has raised a demand to develop a new program, specifically design to reduce the drawbacks of both previous roads. The requirements for this new program are the goals of this dissertation thesis. These goals are to develop a program, that will:

- be used in design and analysis of typical thick composite parts,
- predict displacements in one plane,
- calculate the element loads, stresses and strains,
- export these results in understandable fashion,
- be easy and flexible to use,
- allow user to export geometry of deformed body,
- allow user to export NASTRAN BDF file.

Further more this software must be verified and validated.

This dissertation thesis begins with overview of current trends in the field of composite part analysis and summarises the relevant research to be incorporated into the developed software. This new software is called KuFEM.

KuFEM is a software tool with own graphical user interface. Data inputs are made with spreadsheet tables, therefore in a very simple, understandable and user-friendly way, which allows dynamic and flexible workflow. Managing data inputs in this way saves time and allows user to efficiently try out number of simulations in order to achieve desired results.

Solution for deformed shape calculation is based on a scripts in Matlab programming language, provided by Antonio Ferreira [1]. These codes were modified (cross-section homogenization and multiple beam theory incorporation) and translated to Python programming language, exploiting numpy package. Using Python offers significant advantages: final program can have efficient graphical user interface, can be distributed freely and as a stand-alone executable file.

Further code determining the internal forces, moments stresses and strains are author's original work. So is the non-linear sequence and element description formulation and data export functions (IGES geometry, NASTRAN BDF and Abaqus INP files).

Products, based on KuFEM design, optimization and strain analysis were manufactured as prototypes and tested at TechProAviation s.r.o. First product was nose gear spring (shown in green on figure 5.1). This horse-shoe-shaped spring has been designed, manufactured and tested for stiffness (discussed in chapter 4.3). The product has met the requirements and is now in serial production.



Figure 5.1: Nose gear spring (in green) on Merlin 105 airplane. Courtesy of TechProAviation, s.r.o.

Another product, where KuFEM contributed in design process is tail gear spring. It has been also tested and declared to comply with the requirements. This spring is used on two types: Merlin 110 and Merlin Sportster (shown in green on figure 5.2).



Figure 5.2: Tail gear spring (in green): Merlin Sportster. Courtesy of TechProAviation, s.r.o.

Last product, KuFEM has been used for, is landing gear for an ultralight helicopter called Dropper. The landing gear (shown in green on figure 5.3) has been manufactured and first testing is expected in Q1 of 2018.

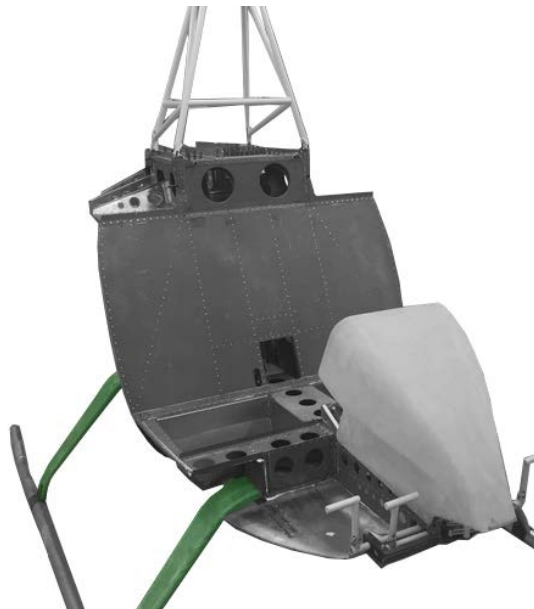


Figure 5.3: Main landing gear (in green) of a helicopter. Courtesy of TechProAviation, s.r.o.

Goals, that were set in chapter 2.4 were met: a software has been developed, verified and validated. Practical results were presented on products of TechProAviation company. Software, that is outcome of this dissertation thesis, is user-friendly, stand-alone and distributed free of charge as an open source project⁹. Intended target users are mainly small companies, developing aeronautical composite components. Other use of KuFEM software can be found in similar applications: automotive industry (leaf springs), sport equipment (bows, jumping stilts) and maritime industry (mast, boom and oar).

A list of further enhancements and potential issues is kept for future development of KuFEM program, which still goes on.

⁹Available at author's personal web page <http://www.cejpek.eu/KuFEM>

References

- [1] Ferreira A., *MATLAB CODES FOR FINITE ELEMENT ANALYSIS*: Solids and Structures. Springer Science & Business Media - Technology & Engineering. 235 pages. 2008. ISBN 1402092008.
- [2] Janíček, Ondráček, Vrbka. *PRUŽNOST A PEVNOST I*. VUT v Brně. 1992.
- [3] MSC.Software. *MSC NASTRAN 2014*: Quick reference guide. 3854 pages. 2014.
- [4] Torstenfelt B., *FINITE ELEMENTS*, Preliminary edition LiU-IEI-S-08/535-SE. Linköping universitet. 2008.
- [5] Liu Y. *INTRODUCTION TO THE FINITE ELEMENT METHOD*. 188 pages. CAE Research Laboratory. 2003.
- [6] Bathe K., *FINITE ELEMENT PROCEDURES FOR SOLIDS AND STRUCTURES*. RES.2-002 Spring 2010. Massachusetts Institute of Technology: MIT OpenCourseWare, <https://ocw.mit.edu>. License: Creative Commons BY-NC-SA.
- [7] Gavin H. *STRUCTURAL ELEMENT STIFFNESS, MASS, AND DAMPING MATRICES*. CEE 541. Structural Dynamics, Duke University, 2016. 33 pages.
- [8] Matthews B. *APPLIED STRESS ANALYSIS* Section XI: Composite Materials (Analysis). General Dynamics, Convair Division, 92 pages.
- [9] Wanga C., Lima G., *RELATIONSHIPS BETWEEN BENDING SOLUTIONS OF REISSNER AND MINDLIN PLATE THEORIES*, Engineering Structures, Volume 23, Issue 7, Pages 838–849, July 2001.
- [10] ANSYS, Inc. *ANSYS 17 Update*. 66 pages. 2016.
- [11] Goering J., Kim H. *HIGHER ORDER FINITE ELEMENT ANALYSIS OF THICK COMPOSITE LAMINATES*. NASA Act NAS1-18862, McDonnell Douglas Corp., St. Louis.
- [12] Bednarczyk B., Aboudi J. *SIMPLIFIED SHEAR SOLUTION FOR DETERMINATION OF THE SHEAR STRESS DISTRIBUTION IN A COMPOSITE PANEL FROM THE APPLIED SHEAR RESULTANT*. American Institute of Aeronautics and Astronautics. 25 pages. 2008.
- [13] Bathe K. *INTRODUCTION TO NONLINEAR ANALYSIS*. [online 2017-01-13] available at <https://youtu.be/TJh7KPABk6I>
- [14] Quora *What is the difference between displacement, deflection and deformation?*. [online 2017-03-10] available at <https://www.quora.com/What-is-the-difference-between-displacement-deflection-and-deformation>
- [15] Department of Defense Handbook *COMPOSITE MATERIALS HANDBOOK*: volume 3. polymer matrix composites materials usage, design and analysis. Washington D.C. 2012. 693 pages. MIL-HDBK-17-3F.
- [16] Hussain S., *PREDICTION OF ELASTIC PROPERTIES OF FRP COMPOSITE LAMINA FOR LONGITUDINAL LOADING*. 6 pages. ARPN Journal of Engineering and Applied Sciences, 2008.
- [17] Samborsky D., *3-D STATIC ELASTIC CONSTANTS AND STRENGTH PROPERTIES OF A GLASS/EPOXY UNIDIRECTIONAL LAMINATE*. 26 pages. Montana State University, Bozeman, MT 59717.
- [18] Kaw A., *MECHANICS OF COMPOSITE MATERIALS*. 473 pages. Florida 2006. ISBN 0-8493-1343-0.

- [19] Thirumalai R., Andersen L. *TENSILE AND COMPRESSION PROPERTIES OF HYBRID COMPOSITES – A COMPARATIVE STUDY*. In Proceedings of the 19th International Conference on Composite Materials (ICCM19). (pp. 1029-1035). Canadian Association for Composite Structures and Materials. 2013.
- [20] Davallo M., Pasdar H. *EFFECTS OF LAMINATE THICKNESS AND PLYSTACKING SEQUENCE ON THE MECHANICAL PROPERTIES AND FAILURE MECHANISM OF UNIDIRECTIONAL GLASS-POLYESTER COMPOSITES*. International Journal of ChemTech Research, Vol.2, No.4, pp 2118-2124. ISSN : 0974-4290. 2010.
- [21] Spencer E. *A NOVEL OPTIMIZATION STRATEGY FOR COMPOSITE BEAM TYPE LANDING GEAR FOR LIGHT AIRCRAFT*. 24 pages. United Technologies Aerospace Systems, [online 2016-12-16] available at http://pages.mscsoftware.com/rs/mscsoftware/images/Paper_ANoveOptimizationStrategyforCompositeBeamTypeLandingGearforLightAircraft.pdf
- [22] Goyal A., *DESIGN, ANALYSIS AND SIMULATION OF A COMPOSITE MAIN LANDING GEAR FOR A LIGHT AIRCRAFT*. 6 pages. MSRSAS Bangalore. 2002.
- [23] Ilic I., *STRENGTH ANALYSIS OF MAIN LANDING GEAR TYPE LAYERED COMPOSITE LEAF SPRING FOR UNMANNED AERIAL VEHICLE*. 4 pages. Military Technical Institute, Belgrade. 2012.
- [24] ASTM Int., *F 2245-07*. Standard Specification for Design and Performance of a Light Sport Airplane.
- [25] Letecká amatérská asociace ČR, *UL2 - I. ČÁST*. Požadavky letové způsobilosti SLZ. 51 pages. 2002.
- [26] Deutsche Flugsicherung, *NACHTRICHTEN FUR LUFTFAHRER*, teil II. 42 pages. 2003.
- [27] EASA, *CS-22*, Certification specifications for sailplanes and powered sailplanes. 140 pages. 2003.
- [28] Juračka J. *KOMPOZITNÍ KONSTRUKCE V LETECTVÍ*. 103 pages. Brno University of technology, 2007. LU31-2007-OST.ST.
- [29] Schoř P. *ADVANCES IN COMPOSITE STRUCTURES DESIGN AND SIMULATION*, training modules for Researchers, Volume 3. Brno University of technology. 60 pages. 2015.
- [30] Cejpek J. *NAPĚŤOVĚ-DEFORMAČNÍ ANALÝZA SEGMENTU KOMPOZITOVÉHO KŘÍDLA*. 10 pages. Setkání uživatelů MSC.Software s.r.o. 2013. ISBN 978-80-260-4173-3.
- [31] Cejpek J., Juračka J. *MODIFICATIONS OF A SIMPLE I- BEAM AND ITS EFFECTS ON THE STRESS STATE*. Aviation, 2016, 20, 4 pages 168-172. ISSN: 1648-7788.
- [32] Cejpek J., Weis, M., Juračka, J. *ACOUSTIC EMISSION LOCALIZATION IN TESTING OF COMPOSITE STRUCTURES*. Applied Mechanics and Materials, Vol. 821, pp. 405-411, 2016
- [33] Numpy community *NUMPY REFERENCE RELEASE 1.11.0*. [online 2016-12-18] available at <https://docs.scipy.org/doc/numpy-1.11.0/numpy-ref-1.11.0.pdf>
- [34] wxpython [online 2016-12-18] available at <https://wxpython.org/>
- [35] py2exe [online 2016-12-18] available at <http://www.py2exe.org/>

Curriculum Vitae

Personal information

- Name: Jakub Cejpek
- Residence: Brno
- Email: jakub@cejpek.eu
- Year of birth: 1987

Education

- Bachelor degree, 2006-2009, Brno University of technology
- Masters degree, 2009-2011, Brno University of technology

Publications

- Cejpek J. *Napětově-deformační analýza segmentu kompozitového křídla*. 10s. Setkání uživatelů MSC.Software s.r.o. 2013. ISBN 978-80-260-4173-3.
- Cejpek J., Juračka J. *Modifications of a simple I-beam and its effects on the stress state*. Aviation, 2016, 20, 4, pages 168-172. ISSN: 1648-7788.
- Cejpek, J.; Weis, M.; Juračka, J. *Acoustic emission localization in testing of composite structures*. Applied Mechanics and Materials, Vol. 821, pp. 405-411, 2016
- Cejpek, J. *Design of composite landing gear for an LSA airplane* Aircraft Engineering and Aerospace Technology Vol 90 iss.1, ISSN 0002-2667, 2018.

University Projects

- Stress-strain deformation of chosen airplane composite parts, 2011.
- Analysis of airplane structures compression loaded and acoustic localization of a damage in composite materials, 2013.
- Design of a composite spherical projection wall R2, +45°-45°H, 225V, 2014.

TechProAviation Projects where KuFEM has been used

- Merlin 100 main landing gear spring
- Merlin 100 nose gear spring
- Merlin 110 tail gear spring
- Merlin Sportster main gear spring
- Dropper main gear spring

Abstract

Relatively large number of private companies in the Czech Republic are producing light sport aircraft. Significant number of these airplanes use composite landing gear springs. These springs are either smaller parts that absorb energy (nose and tail gear springs) or they can be used for the main landing gear.

All these types of springs share very similar characteristics: they are made mostly of unidirectional composite of significant thickness, the main loading character is bending moment and large deformations are expected. In fact the wing main spar shares similar characteristic.

How are these products designed and analysed? Generally there are two possibilities. First possible way, to design such product, is to make just a simple analysis (closed-form solution, perhaps some spreadsheet table). The drawbacks of this method are limited capabilities and inflexible application. Second option is to perform an analysis study, perhaps even optimization loops in a professional dedicated finite element program. Of course the drawback is the price (for the program and for the engineer).

This dissertation thesis aims to develop a computer program, that will offer third possibility: thorough analysis of given products without expensive software. This program will simplify and speed up the design and strength analysis. It will allow user to quickly test different variants. Specifics of the targeted products (such as large deformations, local through-thickness stress concentrations and wrap plies) will be taken into account.

From the user's point of view the program should be simple to work with. Minimum input data with clear graphical user interface layout ensures comfortable use. Having a stand alone program (executable without any supplementary software) improves the distribution potential.

Abstrakt

Poměrně velké množství soukromých firem v České republice vyrábí lehká sportovní letadla. Značná část těchto letadel využívá kompozitní pružiny ve svých přistávacích zařízeních. Tyto pružiny jsou buďto menší díly, absorbující energii (na přídové noze či ostruže), anebo jde celé pružnice hlavního podvozku.

Všechny tyto pružiny sdílí základní charakteristiky: jsou vyrobeny převážně z jednosměrného kompozitu s významnou tloušťkou, hlavním druhem zatížení je ohybový moment a jsou očekávány velké deformace. Podobnou charakteristiku můžeme použít i při popisu hlavního nosníku křídla.

Jak vypadá návrh a analýza takovýchto dílů? V zásadě jsou dvě možnosti. První z nich je poměrně jednoduchá analytická analýza, případně naprogramovaná v tabulkovém výpočetním prostředí. Nevýhody tohoto řešení jsou limitované možnosti výpočtu a jeho nízká flexibilita. Druhou možností je využít komerční konečno-prvkový systém pro analýzu, případně i pro optimalizaci. Pochopitelnou nevýhodou této možnosti je cena programu a obsluhy.

Cílem této disertační práce je vytvořit program, jež nabídne třetí možnost, která umožní provádět zevrubnou analýzu řešených produktů bez nutnosti pořizovat nákladný software. Tento program zjednoduší a urychlí návrh a pevnostní kontrolu. Umožní uživateli rychle analyzovat více návrhových variant. Program dále bude zohledňovat specifika analyzovaných produktů (například velké deformace a lokální koncentrace napětí kolmo na vlákno).

Z pohledu uživatele by program měl být jednoduchý na ovládání. Minimum množství vstupních dat a přehledné grafické rozhraní zajistí komfortní používání. Samostatně spustitelný program (bez instalace a bez podpůrného softwaru) zlepšuje rozšiřitelnost programu.